Improved semi-experimental equilibrium structure and high-level theoretical structures of ketene ©FREE

Houston H. Smith ⁽¹⁾; Brian J. Esselman ⁽¹⁾; Samuel A. Wood ⁽¹⁾; John F. Stanton ¹² ⁽¹⁾; R. Claude Woods ¹² ⁽¹⁾; Robert J. McMahon ¹² ⁽¹⁾



J. Chem. Phys. 158, 244304 (2023) https://doi.org/10.1063/5.0154770





CrossMark





Cite as: J. Chem. Phys. 158, 244304 (2023); doi: 10.1063/5.0154770

Submitted: 15 April 2023 • Accepted: 25 May 2023 •

Published Online: 23 June 2023







Houston H. Smith, Derian J. Esselman, Description Samuel A. Wood, Description John F. Stanton, and Robert J. McMahon Description

AFFILIATIONS

- Department of Chemistry, University of Wisconsin-Madison, Madison, Wisconsin 53706, USA
- ²Quantum Theory Project, Departments of Physics and Chemistry, University of Florida, Gainesville, Florida 32611, USA
- a) Authors to whom correspondence should be addressed: johnstanton@chem.ufl.edu; rcwoods@wisc.edu; and robert.mcmahon@wisc.edu

ABSTRACT

The millimeter-wave rotational spectrum of ketene ($H_2C=C=O$) has been collected and analyzed from 130 to 750 GHz, providing highly precise spectroscopic constants from a sextic, S-reduced Hamiltonian in the I^r representation. The chemical synthesis of deuteriated samples allowed spectroscopic measurements of five previously unstudied ketene isotopologues. Combined with previous work, these data provide a new, highly precise, and accurate semi-experimental (r_e) structure for ketene from 32 independent moments of inertia. This r_e structure was determined with the experimental rotational constants of each available isotopologue, together with computed vibration-rotation interaction and electron-mass distribution corrections from coupled-cluster calculations with single, double, and perturbative triple excitations [CCSD(T)/cc-pCVTZ]. The 2σ uncertainties of the r_e parameters are ≤ 0.0007 Å and 0.014° for the bond distances and angle, respectively. Only S-reduced spectroscopic constants were used in the structure determination due to a breakdown in the A-reduction of the Hamiltonian for the highly prolate ketene species. All four r_e structural parameters agree with the "best theoretical estimate" (BTE) values, which are derived from a high-level computed r_e structure [CCSD(T)/cc-pCV6Z] with corrections for the use of a finite basis set, the incomplete treatment of electron correlation, relativistic effects, and the diagonal Born–Oppenheimer breakdown. In each case, the computed value of the geometric parameter lies within the statistical experimental uncertainty (2σ) of the corresponding semi-experimental coordinate. The discrepancies between the BTE structure and the r_e structure are 0.0003, 0.0000, and 0.0004 Å for r_{C-C} , r_{C-H} , and r_{C-O} , respectively, and 0.009° for θ_{C-C-H} .

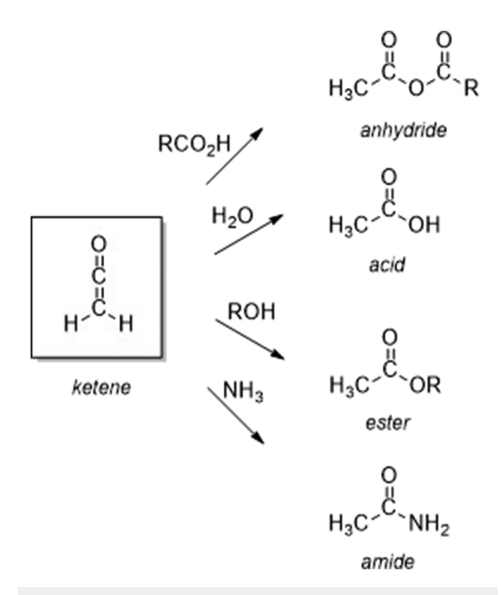
Published under an exclusive license by AIP Publishing. https://doi.org/10.1063/5.0154770

INTRODUCTION

Ketenes (R₂C=C=O) represent an important functional group in organic chemistry. ^{1,2} The reactivity of ketenes, albeit modulated by the nature of the substituents, is generally very high with respect to cycloaddition reactions and the addition of nucleophiles. As such, ketenes are precursors to the family of carboxylic acid derivatives, including anhydrides, carboxylic acids, esters, and amides (Scheme 1). It is the central relationship to these and other functional groups that places ketenes as important intermediates in diverse areas of science, including synthetic organic chemistry, ¹⁻³ petroleum refining, ⁴ photolithography, ⁵ atmospheric chemistry, ⁶

combustion, and astrochemistry. The parent molecule of the family, ketene ($H_2C=C=O$), is a paradigm in terms of structure, bonding, and reactivity. It is a cornerstone of structural organic chemistry and has attracted substantial interest from both experimental and theoretical communities. In the current study, we describe the determination of a highly precise, gas-phase molecular structure for ketene using state-of-the-art methods for both experiment and theory.

Ketene (H₂C=C=O, C_{2 ν}, ethenone) has been identified as an interstellar molecule, with its initial detection in Sgr B2 in 1977. Its detection in that source was later confirmed, ¹⁰ and various subsequent studies detected ketene in other galactic ^{11–15} and extragalactic ¹⁶ sources. Ketene has been generated from the photolysis



SCHEME 1. Reactions of ketene with various nucleophiles.

of interstellar ice analogs comprising a variety of chemical compositions (O₂ + C₂H₂, CO₂ + C₂H₄, CO + CH₄).⁸ The central, electrophilic carbon atom of ketene reacts with common interstellar molecules H2O, NH3, CH3OH, and HCN to form acetic acid, acetamide, methyl acetate, and pyruvonitrile, respectively.¹⁷ of these reaction products have potential prebiotic importance in the interstellar medium. Ketene can also be generated from the decomposition of two known interstellar molecules: acetic acid²⁰ and acetone.²¹ The acylium cation $(H_3C-C\equiv O^+, C_{3\nu})$,²² which has recently been detected in the ISM,²³ is a protonated form of ketene. Due to its prevalence and possible role in the chemical reactions of extraterrestrial environments, the observation of rotational transitions of ketene in its ground and vibrationally excited states is important to radioastronomers. Previously, the rotational spectra of various ketene isotopologues have been observed and assigned up to a frequency of 350 GHz. In this work, we extended the frequency range to 750 GHz for 15 ketene isotopologues, including all singly substituted heavy-atom isotopologues of ketene, ketene d_1 , and ketene- d_2 . The doubling of the spectral range for ketene isotopologues, along with new isotopologue analyses, expands the capabilities for radioastronomers to search for ketene spectral lines in different extra-terrestrial environments.

The pure rotational spectra of ketene and its isotopologues have been extensively studied for over seventy years. The rotational spectrum of ketene and its two deuteriated isotopologues, [2-²H]-ketene (HDC=C=O) and [2,2-²H]-ketene (D₂C=C=O), were measured in the early 1950s. ^{24,25} Subsequently, heavy-atom substituted isotopologues [2-¹³C]-ketene and [¹⁸O]-ketene were measured in 1959 and 1963, ^{26,27} but the final single-substitution isotopologue, [1-¹³C]-ketene, was not reported until 1990. ²⁸ In 1966, the proton spin–rotation and deuterium nuclear quadrupole constants were determined for ketene, [2-²H]-ketene, and [2,2-²H]-ketene. ²⁹ In 1976, the frequency range was extended into the millimeter-wave region (up to 220 GHz) for [2-²H]-ketene and

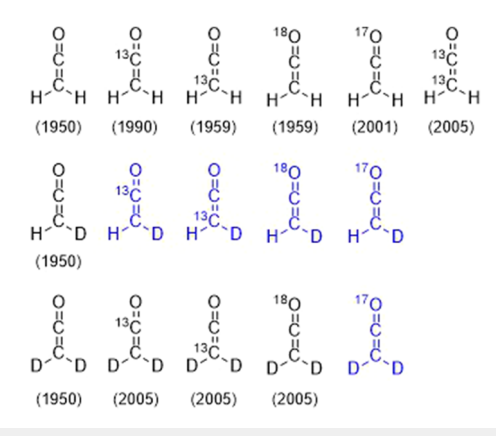


FIG. 1. Ketene isotopologues previously measured (black) and newly measured in this work (blue). Ketene, [2-²H]-ketene, and [2,2-²H]-ketene were measured by Bak *et al.*²⁴ [2-¹³C]-ketene and [¹⁸O]-ketene were measured by Cox *et al.*²⁶ [1-¹³C]-ketene was measured by Brown *et al.*²⁸ [1⁷O]-ketene was measured by Guarnieri and Huckauf³¹ [1,2-¹³C]-ketene, [2,2-²H, 1-¹³C]-ketene, and [2,2-²H, ¹⁸O]-ketene were measured by Guarnieri.³² The date listed indicates the first literature report of that isotopologue.

[2,2- 2 H]-ketene, permitting analysis of their centrifugal distortion. More recent studies expanded the measured frequency range to 350 GHz for various isotopologues, refined the least-squares fits, and measured the spectra of new isotopologues [17 O]-ketene, 31 [1,2- 13 C]-ketene, 32 [2,2- 2 H, 1- 13 C]-ketene, 32 [2,2- 2 H, 2- 13 C]-ketene, 32 and [2,2- 2 H, 18 O]-ketene. For ketene, itself, Nemes *et al.* reported the measurement of 82 *a*-type, $\Delta K_a = 0$ transitions up to 800 GHz. Figure 1 shows the 11 isotopologues for which rotational spectra have previously been reported (black) and the five isotopologues newly measured in this work (blue).

The gas-phase infrared spectrum of ketene was recorded nearly 85 years ago.³⁴ The rotational structure in the infrared spectrum was first analyzed by Halverson and Williams,³⁵ followed by Harp and Rasmussen,³⁶ Drayton and Thompson,³⁷ Bak and Andersen,³⁸ and Butler et al.39 The infrared spectra of [2-2H]-ketene and [2,2-2H]-ketene were reported in 1951,40 and the first vibrationrotation bands of ketene and [2,2-2H]-ketene were observed by Arendale and Fletcher in 1956. 41,42 The first complete analysis of the rotationally resolved infrared spectra of the nine fundamental states present in ketene, [2-2H]-ketene, and [2,2-2H]-ketene was performed by Cox and Esbitt in 1963.⁴³ Nemes explored the Coriolis coupling present in v_5 , v_6 , v_8 , and v_9 of ketene in two separate studies in 1974 and 1978. ^{44,45} A similar study was done on $[2,2^{-2}H]$ -ketene by Winther et al., where v_5 , v_6 , v_8 , and v_9 were examined. 46 A high-resolution infrared analysis of the four A₁ vibrational states for ketene, [2-2H]-ketene, and [2,2-2H]-ketene was performed by Duncan et al., 47 followed by the high-resolution infrared study of v_5 , v_6 , v_7 , and v_8 fundamental states and two overtone states for ketene by Duncan and Ferguson.⁴⁸ The v_9 , v_6 , and v_5 bands in [2,2-2H]-ketene were analyzed with high-resolution infrared spectroscopy by Hegelund et al. 49 Escribano et al. 50 examined the v₁ band of ketene in 1994, which is coupled to other vibrational modes. The fundamental states, v_5 and v_6 , were re-examined by Campiña et al.⁵¹ in 1998 along with the observation of $v_6 + v_9$ in 1999 by Gruebele et al.⁵² Johns et al.⁵³ were able to update the ground-state

spectroscopic constants derived from millimeter-wave data along with the infrared data provided by Campiña *et al.*⁵¹ and Escribano *et al.*⁵⁰ Nemes *et al.*⁵⁴ revisited the non-linear least-squares fitting of v_5 , v_6 , and v_9 and were able to remove most of the Coriolis perturbation contributions to the A_{ν} rotational constants and derive new experimental Coriolis ζ constants. The vibrational energy manifold

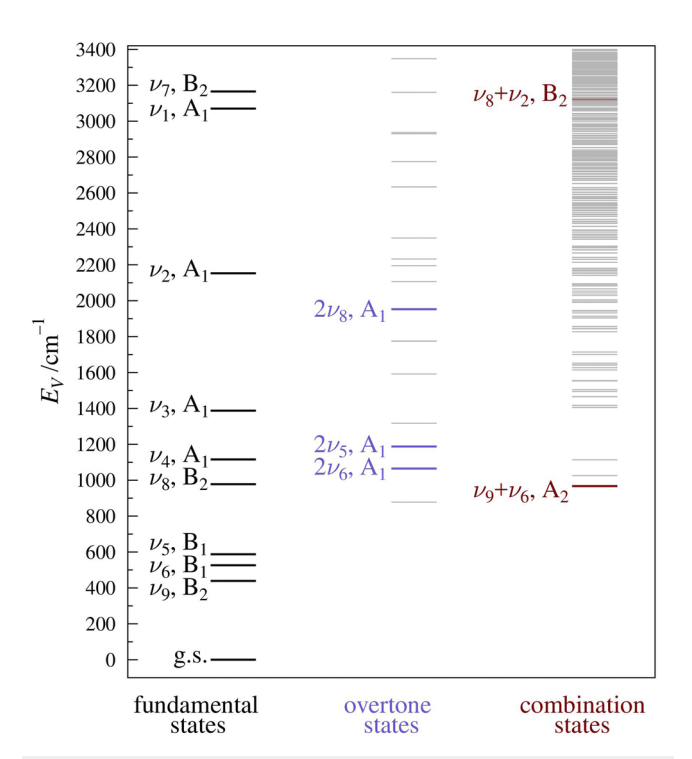


FIG. 2. Vibrational energy levels of ketene below 3400 cm⁻¹. Experimentally observed vibrational energy levels (black, purple, and maroon) are each taken from the most recent literature report and labeled. 44-54 Unobserved vibrational energy levels (gray) are depicted using the computed fundamental frequencies [CCSD(T)/cc-pVTZ]. Overtone and combination states are provided up to five quanta.

up to 3400 cm⁻¹ is shown in Fig. 2, using the experimental frequencies where available and supplementing with computed values where experimental values are not available.

The observation and assignment of various ketene isotopologues have been used for several structural determinations presented in Table I.^{28,55–58} The first zero-point average structure (r_z) , accounting for harmonic vibrational corrections, centrifugal distortion, and electronic corrections, was determined in 1976.⁵⁵ A second r_z structure was calculated in 1987, 56 after several studies examining the vibrational spectra of ketene isotopologues facilitated a more physically realistic general harmonic force field to be applied to the structure calculation. 47,48,59 The additional measurement of [1-13C]-ketene by Brown et al.28 enabled the first complete substitution structure (r_s) determination, where every atom was isotopically substituted at least once in the structure determination. The first semi-experimental equilibrium structure (r_e^{SE}) , using vibration-rotation interaction corrections calculated from an anharmonic force field, was calculated in 1995 with the rotational constants of the six isotopologues available at that time.⁵⁷ The six isotopologues in this r_e^{SE} structure provide 12 independent moments of inertia, which is more than sufficient to determine the four structural parameters of ketene. Guarnieri et al. 31,32,60 measured and assigned rotational transitions for five new isotopologues and determined an updated r_e^{SE} from the rotational constants of 11 isotopologues (22 independent moments of inertia) using vibration-rotation corrections calculated at the MP2/cc-pVTZ level in 2010. 58 The two $r_e^{\rm SE}$ structures are generally in good agreement but disagree somewhat with respect to the r_{C-H} value.

The foundation for semi-experimental equilibrium $(r_e^{\rm SE})$ structure determination was pioneered by Pulay, Meyer, and Boggs, ⁶³ and the accuracy of the structures obtained using this approach has been exemplified in various studies. ^{64–67} The accuracy of semi-experimental structures using different computational methods was investigated in the 1990s and $2000s^{68-74}$ and was comprehensively reviewed by Puzzarini⁷⁵ and Puzzarini and Stanton. ⁷⁶ The coupled-cluster method for both geometry optimizations and anharmonic force-field calculations, along with sufficiently large basis sets for the molecule of interest, was shown to provide the most accurate structural parameters. ^{73,77} For larger molecules, where coupled-cluster methods are not feasible, structural parameters derived from density

TABLE I. Select previously reported structures of ketene.

	Mallinson and Nemes ⁵⁵ r_z 1976	Duncan and Munro ⁵⁶ r_z 1987	Brown <i>et al.</i> ²⁸ <i>r_s</i> 1990	East et al. ⁵⁷ $r_e^{\text{SE}} 1995$	Guarnieri <i>et al.</i> ⁵⁸ r_e^{SE} 2010
$r_{\text{C-C}}$	1.3171 (20) ^a	1.316 5 (15) ^b	1.314 (72) ^c	1.312 12 (60) ^d	1.3122 (12) ^d
$r_{\mathrm{C-H}}$	$1.0797 (10)^{a}$	$1.080\ 02\ (33)^{b}$	$1.0825 (15)^{c}$	$1.07576(14)^{d}$	$1.0763 (2)^{d}$
$r_{\text{C-O}}$	$1.1608 (20)^a$	$1.161 ext{ 4 } (14)^{b}$	$1.162 (72)^{c}$	$1.160\ 30\ (58)^{d}$	$1.1607 (12)^{d}$
$\theta_{ ext{C-C-H}}$	119.02 (10) ^a	119.011 (31) ^b	118.72 (5) ^c	119.110 (12) ^d	119.115 (22) ^d
$N_{ m iso}^{ m e}$	5	5	6	6	11

^aUncertainties as stated in Mallinson and Nemes.⁵

^b3σ values.

^cUncertainties estimated as recommended by Costain⁶¹ and Harmony et al.⁶²

 $^{^{\}rm d} \text{All}$ statistical uncertainties adjusted from previous reports to be 2σ values.

^eNumber of isotopologues used in the structure determination.

functional methods, e.g., B3LYP/SNSD, display reasonable accuracy.⁷⁸ A number of our recent studies have shown remarkable agreement of CCSD(T)/cc-pCV5Z or CCSD(T)/cc-pCV6Z r_e structures with r_e^{SE} structures determined using CCSD(T)/cc-pCVTZ vibration-rotation corrections. 79-86 The small number of atoms in ketene allows the coupled-cluster approach to be utilized in this work, affording an $r_e^{\rm SE}$ structure of similar precision and accuracy to those recent studies.

EXPERIMENTAL METHODS

The rotational spectra of synthesized samples of ketene and deuteriated ketene, described later, were continuously collected in the segments 130-230, 235-360, 350-500, and 500-750 GHz. The instrument covering the 130-360 GHz range has previously been described. 87-89 The 350-500 and 500-750 GHz segments were obtained with a newly acquired amplification and multiplication chain. VDI Mini SGX (SGX-M) signal generator, with external multipliers WR4.3X2 and WR2.2X2, generates 350-500 GHz and, with external multipliers WR4.3X2 and WR1.5X3, generates 500-750 GHz. These spectral segments were detected by using VDI zero-bias detectors WR2.2ZBD and WR1.5ZBD, respectively. The complete spectrum from 130 to 750 GHz was obtained using automated data collection software over ~12 days with these experimental parameters: 0.6 MHz/s sweep rate, 10 ms time constant, and 50 kHz AM and 500 kHz FM modulation in a tone-burst design. 90 The frequency spectra were combined into a single spectral file using Assignment and Analysis of Broadband Spectra (AABS) software. Pickett's SPFIT/SPCAT programs⁹³ were used for least-squares fits and spectral predictions, along with Kisiel's PIFORM, PLANM, and AC programs for analysis. 94,95 Additional short-frequency ranges of the spectrum were collected with an increased number of scans for low-abundance isotopologues. In our least-squares fits, we assume a uniform 50 kHz frequency measurement uncertainty for our measured transitions, 50 kHz for literature values that did not specify an uncertainty, and 25 kHz for transitions reported by Guarnieri et al.31,32,60 Least-squares fitting output files are provided in the supplementary material.

In this study, we measured and assigned the rotational spectrum from 130 to 750 GHz for the primary (Fig. 3) and deuteriumsubstituted ketene isotopologues, including their heavy-atom

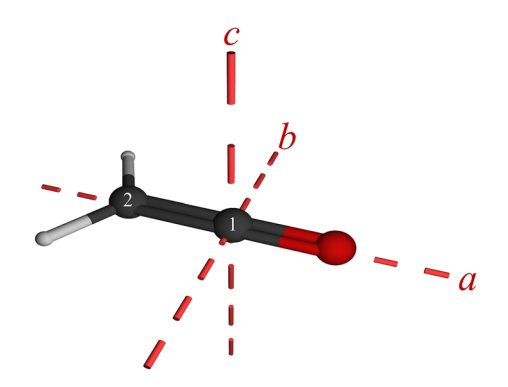


FIG. 3. Ketene structure with principal inertial axes and carbon atom numbering.

isotopologues, $^{13}\mathrm{C}$ and $^{18}\mathrm{O}.$ All $^{17}\mathrm{O}\text{-substituted}$ isotopologues, including the new detection of [2- $^2\mathrm{H},~^{17}\mathrm{O}]\text{-ketene}$ and [2,2- $^2\mathrm{H},$ ¹⁷O]-ketene, were measured from 230 to 500 GHz. The reduced frequency coverage is due to lower signal-to-noise ratios (S/N)for the hardware configurations outside that range. Transitions of [1,2-13C]-ketene could not be measured or assigned due to the proximity of its transitions to those of [2-13C]-ketene and the inherently lower S/N for an isotopologue ~0.0121% the intensity of the main isotopologue. Thus, we were unable to improve upon the spectroscopic constants presented by Guarnieri.³² Due to the planarity condition, each isotopologue provides two independent moments of inertia. With 16 isotopologues used for the new structure determination, an r_e^{SE} structure for ketene was obtained by using 32 independent moments of inertia.

COMPUTATIONAL METHODS

Calculations were carried out using a development version of CFOUR.⁹⁶ The ketene structure was first optimized at the CCSD(T)/cc-pCVTZ level of theory. The optimized geometry and the same level of theory were subsequently used for an anharmonic, second-order vibrational perturbation theory (VPT2) calculation, wherein cubic force constants are evaluated using analytical second derivatives at displaced points. 97-99 Magnetic property calculations were performed for each isotopologue to obtain the electron-mass corrections to the corresponding rotational constants. The "best theoretical estimate" (BTE), as described previously, is based on a CCSD(T)/cc-pCV6Z optimized structure with four additional corrections ' that address the following:

- Residual basis set effects beyond cc-pCV6Z.
- Residual electron correlation effects beyond the CCSD(T)
- Effects of scalar (mass-velocity and Darwin) relativistic
- The fixed-nucleus approximation via the diagonal Born-Oppenheimer correction.

The equations used to calculate these corrections and the values of each of these corrections for ketene are provided in the supplementary material (S7-S13 and Table S-V). One of the most important factors of the algorithm used to determine the BTE is the estimation of residual basis set effects, specifically estimated as the difference between the (directly computed) cc-pCV6Z geometry at the CCSD(T) level of theory and the estimate of the CCSD(T) geometry at the basis set limit. Following others, 100 the latter is estimated by assuming an exponential convergence pattern with respect to the highest angular momentum basis functions present in the basis. A complete explanation of the BTE calculation is provided in the supplementary material.

The xrefit module of CFOUR calculates the moments of inertia and the semi-experimental equilibrium structure using the experimental, S-reduced rotational constants and computational electron-mass distribution and vibration-rotation corrections. The xrefiteration program was used to reveal insight into the contributions of additional isotopologues in refining the structure.⁸² The routine begins by determining a structure using a single isotopic substitution at each position and then sequentially adding the most uncertainty-minimizing isotopologue to the structural least-squares

SCHEME 2. Ketene isotopologue synthesis: (a) ketene- h_2 by pyrolysis of acetone- h_6 , (b) mixture of ketene isotopologues by pyrolysis of 50% deuterium-enriched acetone, and (c) ketene- d_2 by pyrolysis of acetone- d_6 .

fit until all available isotopologues are incorporated. The routine is also useful in assessing the quality of the fit for each isotopologue, since a problematic fit may be readily apparent as a deviation in the *xrefiteration* plot.

Computational output files are provided in the supplementary material.

SYNTHESIS OF KETENE ISOTOPOLOGUES

Ketene was synthesized by pyrolysis of acetone (HPLC grade, Sigma-Aldrich) at atmospheric pressure using a lamp described by Williams and Hurd¹⁰¹ and collected in a $-130\,^{\circ}$ C cold trap [Scheme 2(a)]. After collection, the cold trap was isolated from the pyrolysis apparatus and placed under vacuum to remove volatile impurities; ketene was then transferred to a stainless-steel cold trap for spectroscopic investigation. A mixed deuterio-/protio-solution of acetone- d_x was produced by a procedure modified from Paulsen and Cooke, ¹⁰² using acetone, D₂O, and lithium deuteroxide (LiOD). The reaction mixture was distilled, yielding \sim 50% deuterium-enriched acetone. Pyrolysis and purification of this mixture produced ketene, [2- 2 H]-ketene, and [2,2- 2 H]-ketene [Scheme 2(b)]. An independent sample of [2,2- 2 H]-ketene [Scheme 2(c)] with high deuterium incorporation was generated by pyrolysis of acetone- d_6 (99.5%, Oakwood Chemical).

ANALYSIS OF ROTATIONAL SPECTRA

The rotational spectrum of ketene is dominated by ${}^aR_{0,1}$ transitions, but a select few low-intensity ${}^aQ_{0,-1}$ transitions were observable in the lower frequency range. Ketene has an *a*-axis dipole, $\mu_a = 1.414$ (10) D,²⁵ and is extremely close to a prolate top $[\kappa = -0.997$ for the main isotopologue, Eq. (1)], which can result in a breakdown of the A-reduction least-squares fit (I^r representation) of the Hamiltonian,

$$\kappa = \left(\frac{2B - A - C}{A - C}\right). \tag{1}$$

The A-reduction breakdown for molecules that approach a spherical top, a prolate top (in the $I^{r/l}$ representation), or an oblate top (in the $III^{r/l}$ representation) has been discussed previously. ^{84,103–108} (The output files of least-squares fitting for each isotopologue to sextic, A- and S-reduction Hamiltonians in the I^r representation are

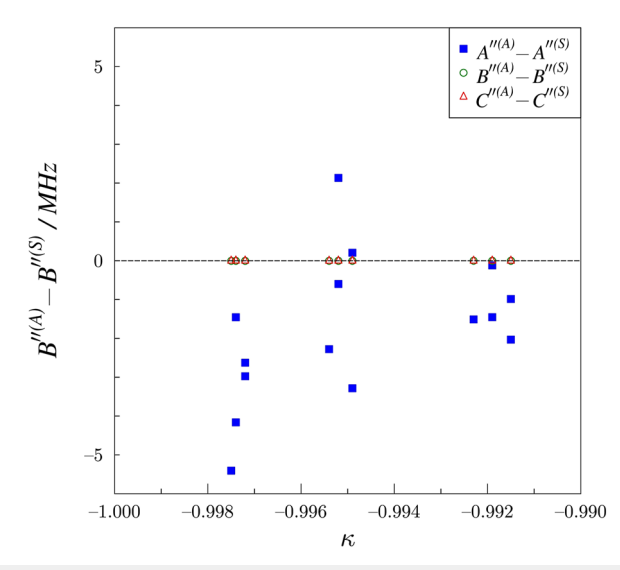


FIG. 4. Difference between the determinable constants (A_0'', B_0'', B_0'') , and $C_0'')$ derived using the A- and the S-reduced Hamiltonians for ketene isotopologues as a function of κ . The symbols for the b- and c-axis differences are so close to zero that they are overlapped and difficult to distinguish on the plot. Note the increase in scatter and the deviation from zero for the a-axis differences as κ approaches the prolate limit of -1.000.

provided in the supplementary material.) For ketene, the experimental and computed A-reduction spectroscopic constants do not appear to display the unreasonably large K-dependent centrifugal distortion constants that have been noted in other cases where the A-reduction breaks down. There is, however, a significant difference between the A- and S-reduction determinable constants (Eqs. S1-S6 in the supplementary material) from the least-squares fits in the A- and S-reductions. The κ values for the ketene isotopologues vary from -0.9915 ([2,2- 2 H]-ketene) to -0.9975 ([18 O]-ketene). The greatest discrepancies in the determinable constants occur for the A_0 constant of the isotopologues with the greatest κ values, [¹⁸O]-ketene and [17O]-ketene. Figure 4 shows the differences in the determinable constants (nominal B'' values) in the A- and S-reductions as a function of κ . While the trend does not show a clearly defined behavior, the variability in A_0'' increases as κ approaches the prolate-top limit (-1.000). Additionally, in each case, the A-reduction fits have a larger statistical uncertainty than the S-reduction fits. Doose et al. 109 observed similar issues with $[2,2^{-2}H]$ -ketene ($\kappa = -0.9915$), including high uncertainties and high correlations for some parameters when only pure rotational transitions were used in the least-squares fit. For these reasons, only the S-reduction spectroscopic constants are presented in the main text of this work and used in the r_e^{SE} structure determination. The S-reduction spectroscopic constants for all ketene isotopologues are presented in Table II.

Table II provides the experimental spectroscopic constants in the S-reduction and I^r representation for all 16 ketene isotopologues used in the semi-experimental equilibrium structure determination. The [1,2-¹³C]-ketene spectroscopic constants provided in Table II are those reported by Guarnieri *et al.*³² due to the inability to measure this isotopologue in this work. Table II includes, for the normal isotopologue, the previously determined spectroscopic constants by Guarnieri and Huckauf⁵⁰ and the computed constants

0.047

0.043

0.034

0.030

0.046

Downloaded from http://pubs.aip.org/aip/jcp/article-pdf/doi/10.1063/5.0154770/18014519/244304_1_5.0154770.pdf

9761.237 01 (38) -0.04547(17)9 421.124 72 (37) 2.949 28 (14) -0.12548(11) $[0.0000544]^{d}$ 9145.129 30 (76) 8 719.333 31 (72) 2.699 45 (58) -0.19148(17)-0.06877(30)282 142.0 (40) -0.000319416 760 (1576) -0.0001117 $[0.000025]^{d}$ $[0.000339]^{d}$ 194 243.2 (31) $[2^{2}H,^{18}O]$ 434.455 (47) 2.495 (13) 297.756 (44) 1.948 (11) $[0.000165]^{\circ}$ $[0.000\,586]$ [0.000105] $[20700]^{d}$ $[4040]^{d}$ $[O_8]$ -614.2 (17) $[5850]^{d}$ 238.6 (15) 171 0.041 -0.132961(89)-0.00110(14)-0.04928(11) $[0.0000237]^{d}$ 8 926.177 92 (60) 9 9 6 0 . 9 7 7 8 8 (37) 9 607.139 42 (35) 3.090 08 (35) $[0.0000595]^{d}$ 9373.431 43 (63) 2.827 55 (61) -0.20328(16)-0.00103(12)282 108.1 (26) 2.5876 (91) 17 090 (1276) -0.07565(27) $[0.000\,369]^{d}$ [2-²H, 2-¹³C] 193 984.2 (26) 2.065 5 (83) $[0.000161]^{d}$ 451.182 (36) 315.948 (35) $[0.000653]^{d}$ 0.000118 $[4060]^{d}$ $[20700]^{d}$ $[5850]^{d}$ $[2^{-13}C]$ -603.0 (13) -240.3 (13) 0.041 -0.147875(96)-0.05596(11)0 293.629 59 (44) 9 916.210 87 (44) -0.00111(21)3.279 63 (49) $[0.000\,025\,9]^{d}$ 9 646.687 07 (65) 9 174.260 89 (64) 3.005 29 (64) 282 104.2 (25) -0.22686(15)-0.08375(26)-0.00104(15)15380 (1098) $[0.000444]^{d}$ [2-²H, 1-¹³C] 194256.1 (23) 0.000073476.701 (43) 327.242 (41) 2.976 (13) $0.000195]^{d}$ $0.000767]^{d}$ $[0.000140]^{\circ}$ 2.316 (11) $[3970]^{d}$ $[2070]^{d}$ $[1-^{13}C]$ -673.7(15)[5930]^d -264.6 (15) 209 0.048 204 -0.147726(11)-0.055755(57)-0.226195(49)0.000782 (35) -0.001380(80)0 293.318 94 (24) 9915.903 04 (24) 3.281 23 (30) -0.00125(13)-0.08410(15) $0.0000264]^{d}$ 3.00461(37)2.9142 (89) $[0.0000724]^{d}$ 9 647.065 33 (21) 9 174.643 51 (20) 282 121.6 (18) 17 400 (674) 2.2843 (67) Current work $0.000194]^{d}$ 477.384 (31) $0.000442]^{d}$ 194 292.2 (13) $[0.000139]^{d}$ 328.426 (25) $[20700]^{d}$ $[2890]^{d}$ -254.39 (89) $[4070]^{d}$ -647.7 (11) $[2-^{2}H]$ 307^t 0.037 344 Normal isotopologue 0.000 026 4 0.000 072 4 -0.0004660.000442-0.0509(11)9 960.865 0 (25) -0.1331(27)9 607.055 0 (27) 3.088 1 (21) -0.0433 $[-0.00204]^{c}$ 282 031 (22) $[1,2^{-13}C]$ 451.12 (11) -3545(53)2.07 (23) $CCSD(T)^{b}$ 20 700 -0.1252.80 $[22.840]^{c}$ 3.15 5890 281 680 10 234 9861 477 -711 -506.9 (42) $[5230]^{c}$ 18.7(47)98 Guarnieri et al. 2003ª -0.13467(76)-0.04845(60) $[0.0000624]^{d}$ 3.099 97 (63) 0.00002581^{d} -0.14757(84)10 293.319 63 (81) 9 915.903 93 (80) -0.05621(51)0 013.4722 (14) 9 655.909 6 (13) 3.2804 (18) $[0.000385]^{d}$ 454.371 (92) $-0.00384]^{d}$ 2.561 (89) 282 175 (13) 282 032 (22) 478.27 (11) $[22\,840]^{c}$ [-0.00204]2.27 (21) 3475 (59) [20 700]^d -635.8 (33) $[2870]^{d}$ $[5230]^{c}$ -21.3(46)-526.2 (45) $[0^{17}0]$ 156 0.040 94 L_{JKK} (mHz) L_{JKK} (mHz) L_{JK} (mHz) D_{JK} (kHz) (mHz) D_{JK} (kHz) H_{KJ} (Hz) H_{JK} (Hz) B₀ (MHz) C₀ (MHz) D_K (kHz) A₀ (MHz) B_0 (MHz) C₀ (MHz) $N_{
m lines}^{
m e}$ $\sigma \, ({
m MHz})$ A₀ (MHz) D_K (kHz) H_{JK} (Hz) D_I (kHz) d_1 (kHz) d_2 (kHz) $\sigma \left(\mathrm{MHz} \right)$ D_I (kHz) H_{KJ} (Hz) H_K (Hz) d_1 (kHz) d_2 (kHz) H_K (Hz) $H_I(Hz)$ h_1 (Hz) h_2 (Hz) h₃ (Hz) H_I (Hz) h_2 (Hz) h₃ (Hz) h_1 (Hz)

TABLE II. Spectroscopic constants for ketene isotopologues, ground vibrational state (S-reduced Hamiltonian, I' representation).

TABLE II. (Continued.)

	[2- ² H, ¹⁷ O]	[2,2- ² H]	[2,2- ² H, 1- ¹³ C]	[2,2- ² H, 2- ¹³ C]	[2,2- ² H, ¹⁸ O]	[2,2- ² H, ¹⁷ O]
A ₀ (MHz)	194 260.6 (27)	141 490.38 (28)	141 484.52 (67)	141 483.16 (65)	141 489.40 (85)	141 490.0(10)
$B_0 ({ m MHz})$ $C_0 ({ m MHz})$	9 383.171 5 (13) 8 935.543 1 (13)	9 120.830 67 (17) 8 552.699 81 (16)	9 119.426 58 (65) 8 551.484 44 (71)	8 8 9 0.4 7 3 5 1 (67) 8 3 4 9.8 4 1 3 1 (61)	8 641.838 91 (56) 8 130.053 11 (54)	8 8 6 9 . 0 6 2 1 (17) 8 3 3 0 . 8 8 1 9 (13)
D_{I} (kHz)	2.84576 (51)	2.48404(19)	2.48496 (48)	2.358 60 (38)	2.23474 (43)	2.355 69(55)
D_{JK} (kHz)	312.295 (66)	322.962 (21)	321.967 (38)	310.142 (37)	294.046 (43)	307.799(76)
D_K (kHz)	15140 (840)	5645 (100)	5327 (225)	5373 (209)	5470 (359)	$[2000]^{d}$
d_1 (kHz)	-0.20921(58)	-0.220132(37)	-0.22025(14)	-0.20100(12)	-0.18676(15)	-0.20448(71)
d_2 (kHz)	-0.07596(29)	-0.114212(87)	-0.11415(31)	-0.10309(28)	-0.09366(32)	-0.10311(28)
H_{J} (Hz)	$[0.0000211]^{ m d}$	-0.001690(47)	-0.00163(12)	-0.001558(95)	-0.001436(96)	$[-0.000862]^{d}$
H_{JK} (Hz)	2.162 (37)	2.077 5 (46)	2.0798 (93)	1.8954(93)	1.690 (12)	2.001(43)
H_{KJ} (Hz)	-243.1 (22)	-127.50(80)	-138.4(14)	-124.0(14)	-129.4(15)	-129.1(27)
H_{K} (Hz)	$[4050]^{d}$	[287] ^d	[793] ^d	$[781]^{d}$	$[781]^{d}$	$[784]^{d}$
h_1 (Hz)	$[0.000178]^{ m d}$	$[-0.0000144]^{ m d}$	$[-0.0000146]^{ m d}$	$[-0.0000142]^{d}$	$[-0.000002]^{d}$	$[-0.00000730]^{d}$
h_2 (Hz)	$[0.00058]^{d}$	0.001030(30)	0.00119(12)	0.00066(11)	0.000 700 (97)	$[0.000752]^{d}$
h ₃ (Hz)	$[0.000\ 120]^{ m d}$	$[0.000208]^{ m d}$	$[0.000208]^{ m d}$	$[0.000180]^{ m d}$	$[0.000156]^{ m d}$	$[0.000179]^{ m d}$
$N_{ m lines}^{ m e}$	107	403	221	218	166	88
σ (MHz)	0.040	0.032	0.046	0.045	0.042	0.046

Constants as reported in Ref. 60. Pa, values obtained from Eq. (2) using the computed values for B_e, vibration-rotation interaction, and electron-mass distribution [each evaluated using CCSD(T)/cc-pCVTZ]. Distortion constants computed using

CCSD(T)/cc-pCVTZ. ^cConstant held fixed to value in Ref. 53 as stated by Ref. 60. ^dConstant held fixed at the CCSD(T)/cc-pCVTZ value.

^eNumber of independent transitions.

^fTransitions reported by Brown *et al.*,³⁸ Johnson and Strandberg,³⁸ and Guarnieri and Huckauf⁴⁰ are induded in the least-squares fit. See the supplementary material for transitions used from previous studies for non-standard isotopologues.

[CCSD(T)/cc-pCV6Z] for comparison to the experimental values determined in this work. The CCSD(T) values for all other isotopologues can be found in the supplementary material. Experimental rotational constants B₀ and C₀ determined by Guarnieri and Huckauf⁶⁰ are in exceptional agreement with this work, but A_0 is not in such good agreement. The computed rotational constants are in good agreement with the experimentally determined ones previously reported, with the largest discrepancy being in B_0 (0.58%). Centrifugal distortion constants determined by Guarnieri and Huckauf⁶⁰ are also in excellent agreement with those determined here, with the largest difference in d_2 (0.81%). Neither work was able to determine D_K , but Guarnieri et al. used the previously determined value from Johns et al.,53 while the present work used the CCSD(T) value. The CCSD(T) value was utilized to maintain a consistent treatment with the sextic centrifugal distortion constants, which were also held fixed at the CCSD(T) values since experimental values are not available. The CCSD(T) values for the centrifugal distortion constants display the expected level of agreement with the experimental values, with the largest discrepancy in d_2 (22%). There are only two sextic distortion constants that were determined both in this work and by Guarnieri and Huckauf, 60 H_{JK} and H_{KJ} , and both are in reasonable agreement (28%). H_I was determined in this work, while it was held fixed in Guarnieri and Huckauf, 60 similar to D_K . H_K is held fixed at two different values in the two works for the same reason as D_K . This work held the off-diagonal sextic centrifugal distortion constants, h_1 , h_2 , and h_3 , fixed at their respective CCSD(T) values, while they were held at zero in the previous studies. This difference seemed to negate the need for the two octic centrifugal distortion constants utilized in the previous studies for the frequency range and K_a range measured in this work. The largest relative discrepancy in the CCSD(T) sextic centrifugal distortion constants that were determined is in H_I (63%),

which is not unexpected due to it being orders of magnitude smaller than the other constants.

The band structure for all ketene isotopologues is typical for a highly prolate molecule, with each band corresponding to a singular J''+1 value with different K_a values. The transitions of the band structure lose K_a degeneracy for $K_a = 3$ for all isotopologues, with the protio-isotopologues losing degeneracy in bands at higher frequencies. The current work expanded the range of quantum numbers of the transitions assigned for ketene to include J''+1=7 to 41 and $K_a = 0$ to 5. The breadth of the transitions assigned in this work is shown in Fig. 5, where all transitions newly measured are in black and previously measured transitions are in various colors indicating their source. All ketene isotopologue least-squares fits were limited to transitions with $K_a \le 5$, even though transitions with higher K_a were observed. This is because a single-state, distorted-rotor Hamiltonian was unable to provide a least-squares fit below the assumed measurement uncertainty of 50 kHz when incorporating transitions above $K_a = 5$. This failure of the single-state least-squares fit to model all of the observable transitions is due to coupling between the vibrational ground and excited states that has been extensively studied in the infrared spectra of ketene and summarized in the Introduction. 44-49,51,52,54 Ån analysis of the vibrational coupling is beyond the scope of the current work. The cutoff of $K_a \le 5$ was implemented for all isotopologues to maintain a consistent amount of spectroscopic information. A similar procedure was applied to previous studies with HN3, which also has a ground state coupled to low-energy fundamental states, 110 and was shown to provide an $r_e^{\rm SE}$ structure with complete consistency with the BTE.

The heavy-atom isotopologues of ketene were observed at natural abundance from the synthesized protio-sample of ketene, and only ${}^aR_{0.1}$ transitions could be observed and measured. The

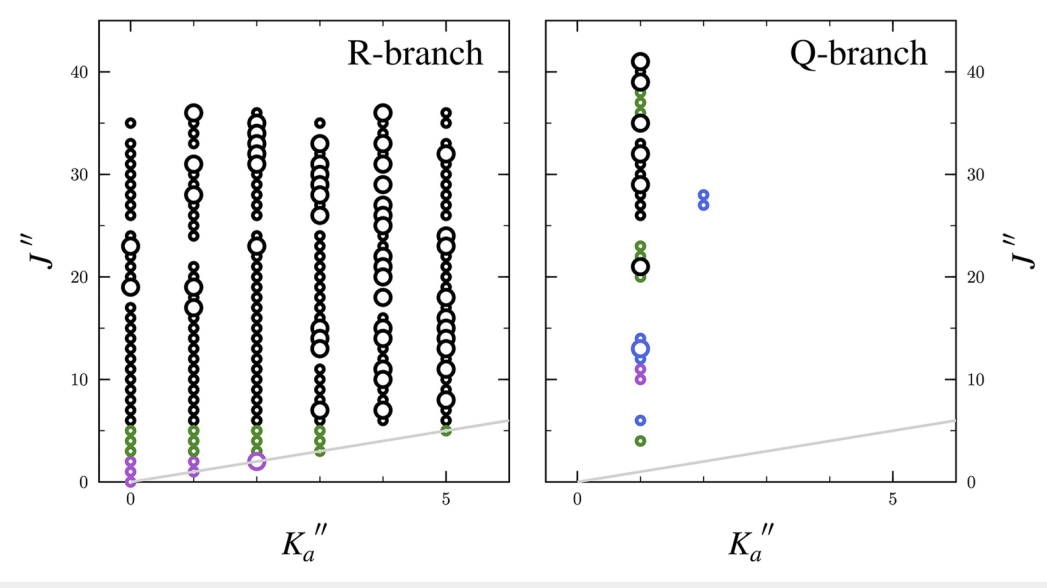


FIG. 5. Data distribution plot for the least-squares fit of spectroscopic data for the vibrational ground state of ketene. The size of the outlined circle is proportional to the value of $|(f_{\text{obs.}} - f_{\text{calc.}})/\delta f|$, where δf is the frequency measurement uncertainty. The transitions are color coordinated as follows: Current work (black), Brown *et al.*²⁸ (purple), Johnson and Strandberg²⁵ (blue), and Guarnieri and Huckauf⁶⁰ (green). Transitions from previous studies that overlapped with current measurements were omitted from the dataset

[2- 2 H]-ketene and [2,2- 2 H]-ketene isotopologues were the only other isotopologues where a Q_{0,-1} transitions could be measured. The [2- 2 H]-ketene isotopologue has a small predicted *b*-dipole moment, $\mu_b = 0.048$ D, but no *b*-type transitions were sufficiently

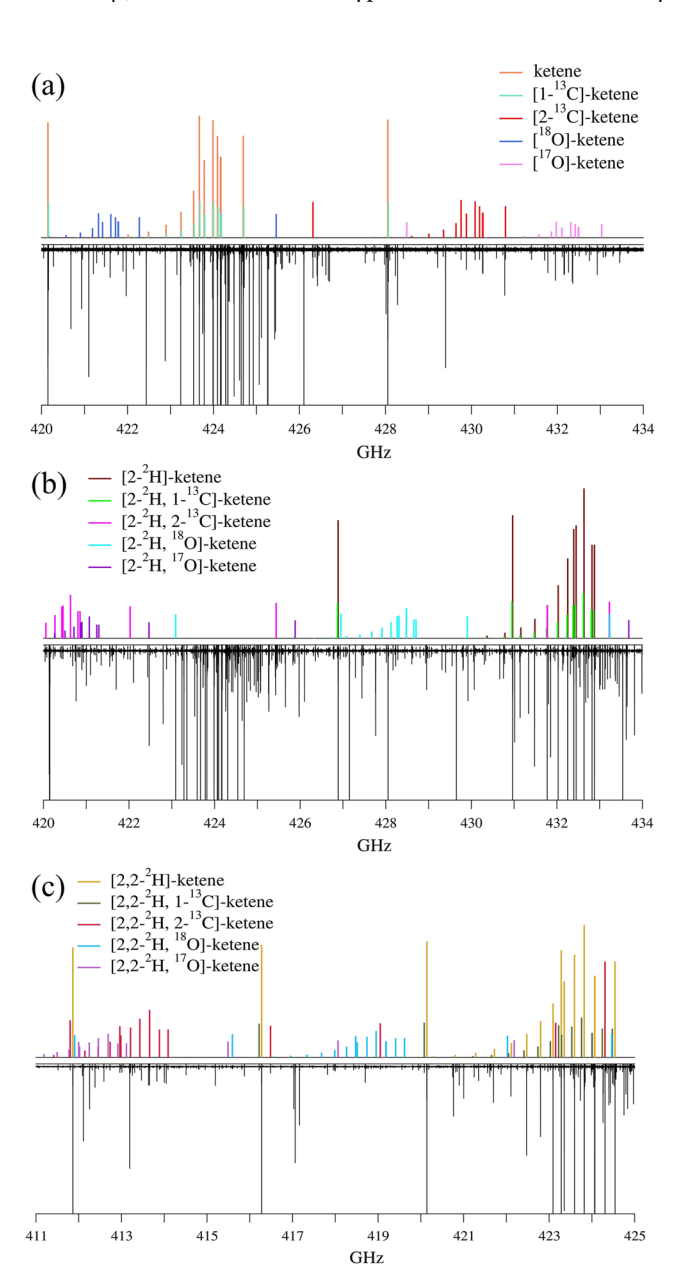


FIG. 6. (a) Stick spectra predicted from experimental spectroscopic constants from 420.0 to 434.0 GHz (top) and experimental spectrum (bottom) of the ketene and heavy-atom isotopologues. (b) Stick spectra predicted from experimental spectroscopic constants from 420.0 to 434.0 GHz (top) and experimental spectrum (bottom) of the [2-²H]-ketene and heavy-atom isotopologues. (c) Stick spectra predicted from experimental spectroscopic constants from 411.0 to 425.0 GHz (top) and experimental spectrum (bottom) of the [2,2-²H]-ketene and heavy-atom isotopologues. Transitions belonging to vibrationally excited states are also discernible.

intense to be observed in our spectrum. All of the heavy-atom isotopologues for [2-2H]-ketene and [2,2-2H]-ketene were observable at natural abundance in their deuterium-enriched samples. For the previously observed isotopologues, the published spectroscopic constants were used as predictions for the spectral region measured in this work. Once rotational constants were obtained for several known isotopologues, a preliminary semi-experimental equilibrium structure was obtained, which provided very accurate equilibrium rotational constants for new isotopologues. Along with CCSD(T) vibrational and electronic corrections and centrifugal distortion constants, the predicted rotational constants were used to assign transitions for the previously unidentified isotopologues: [2-²H, 1-¹³C]-ketene, [2-²H, 2-¹³C]-ketene, [2-²H, ¹⁸O]-ketene, [2-²H, ¹⁷O]-ketene, and [2,2-²H, ¹⁷O]-ketene. This technique greatly expedited the search for these transitions, as the CCSD(T)/ cc-pCVTZ rotational constants predictions were not accurate enough to easily identify and assign the transitions. All heavy-atom isotopologue transitions measured from 500 to 750 GHz and all three ¹⁷O-isotopologues measured from 230 to 500 GHz required averaging 20 scans due to low S/N. These low S/N transitions were collected by acquiring 10 MHz windows around each predicted transition. Despite the various isotopologue substitutions, the spectral pattern (Fig. 6) of ketene was relatively consistent due to the highly prolate nature of the molecule.

The rotational spectra of three separate ketene samples are shown in Fig. 6, where (a) corresponds to the protio-isotopologue from 420 to 434 GHz, (b) corresponds to the $[2^{-2}H]$ -ketene isotopologue from 420 to 434 GHz, and (c) corresponds to the $[2,2^{-2}H]$ -ketene isotopologue from 411 to 425 GHz along with their respective heavy-atom isotopologues. The rotational spectrum of ketene is sparse with the bands of R-branch transitions with constant J values, separated by ~16 GHz or ~2C, allowing for the assignment of multiple isotopologues within one sample spectrum. Thus, there was little issue with transitions overlapping, which would cause a poor determination of the transition frequencies. Each spectrum contains unassigned transitions belonging to excited vibrational states of ketene isotopologues, as shown in Fig. 6. Data distribution plots for the isotopologues, showing the breadth of quantum numbers observed, are provided in the supplementary material.

SEMI-EXPERIMENTAL EQUILIBRIUM STRUCTURE $(r_e^{\rm SE})$

In contrast to several of our recent $r_e^{\rm SE}$ structure determinations, ^{79–86} the spectroscopic constants determined in the S-reduction $(B_0^{\beta(S)})$ were converted to equilibrium constants (B_e^{β}) and used directly in the least-squares fitting of the semi-experimental equilibrium structure without conversion to the determinable constants. In those previous studies, with the exception of $[1,3-^2H]-1H-1,2,4$ -triazole, the A-reduction and S-reduction rotational constants for each isotopologue were converted to the determinable constants from which the centrifugal distortion has been removed. These determinable constants are then averaged before converting to the equilibrium constants (B_e^{β}) for $r_e^{\rm SE}$ structure determination. As noted previously, ketene is an extreme prolate top ($\kappa = -0.997$) with only a-type transitions; thus, the A-reduction spectroscopic constants cannot be determined as

accurately as the S-reduction constants. As a result, the S-reduction specific vibration-rotation interaction corrections determined in the CFOUR anharmonic frequency calculation were used to obtain the equilibrium rotational constants. Thus, the centrifugal distortion corrections used to determine the equilibrium rotational constants are the computed ones rather than the experimental ones. Ideally, the spectroscopic constants would be determined in both the A- and S-reductions, and each rotational constant would be converted to a determinable constant. If the determinable constants were similar, it would give confidence that the rotational and quartic centrifugal distortion constants were determined with sufficient accuracy to be included in the structure determination, regardless of the size of the transition dataset. A similar problem might have arisen in the HN₃ semi-experimental equilibrium structure determinations, 83 but the HN₃ dataset included b-type transitions, along with a-type transitions, which gave enough spectroscopic information to successfully determine the A-reduction spectroscopic constants.

In the current case, the S-reduction rotational constants were input to *xrefit*, along with vibration–rotation interaction and electron-mass distribution corrections predicted at the CCSD(T)/cc-pCVTZ level of theory. The *xrefit* module uses the values to calculate the equilibrium rotational constants (B_e) using Eq. (2), where the second term contains the vibration–rotation interaction correction, $\frac{m_e}{M_p}$ is the electron–proton mass ratio, $B_0^{\beta(S)}$ is the S-reduction rotational constant, and $g^{\beta\beta}$ is the corresponding magnetic g-tensor component,

$$B_e^{\beta} = B_0^{\beta(S)} + \frac{1}{2} \sum_i \alpha_i^{\beta} - \frac{m_e}{M_P} g^{\beta \beta} B^{\beta}.$$
 (2)

These calculated equilibrium rotational constants are then used to calculate the inertial defect (Δ_i) , which is precisely zero for a rigid, planar molecule. For ketene, without either computational correction, the observed inertial defect Δ_{i0} is ~0.09 μ Å² (Table III). Including the vibration-rotation interaction correction decreases the inertial defect to $\sim 0.004 \,\mu\text{Å}^2$, while the inclusion of the electron-mass correction brings the inertial defect to slightly larger than 0.004 μ Å² (Table III) in a similar manner to HN₃.83 These two molecules stand in contrast to the trend observed for heterocyclic molecules, where the vibration-rotation interaction correction results in a small negative value of Δ_{ie} and subsequent application of the electronmass correction brings the magnitude of Δ_{ie} close to zero. The similar inertial defect trend to HN₃ is likely due to the nature of the C-C-O backbone, where the electron mass is more-or-less cylindrically distributed in the combined in-plane and out-of-plane π orbitals.

The semi-experimental equilibrium structure parameters of ketene obtained from 16 isotopologues are shown in Fig. 7 and enumerated in Table IV. The 2 σ statistical uncertainties of the bond distances are all <0.0007 Å, and the corresponding uncertainty in the bond angle is 0.014°. Overall, the precision and accuracy of the structural parameters are similar to those of HN₃⁸³ when comparing the $r_e^{\rm SE}$ calculated at the same level of theory. The 2 σ statistical

TABLE III. Inertial defects (Δ_i) and second moments (P_{bb}) of ketene isotopologues.

Isotopologue	$\Delta_{i0} (\mu \text{Å}^2)^a$	$\Delta_{ie} (\mu \mathring{A}^2)^{a,b}$	$\Delta_{ie} (\mu \text{Å}^2)^{\text{a,c}}$	$P_{bb} (\mu \text{Å}^2)^{c,d}$	$P_{bb}/m_H (\text{Å}^2)^{c,d,e}$
H ₂ CCO	0.0774	0.0035	0.0041	1.782 76	1.768 92
[1- ¹³ C]-H ₂ CCO	0.0772	0.0035	0.0040	1.782 77	1.768 93
$[2^{-13}C]$ -H ₂ CCO	0.0772	0.0035	0.0041	1.782 75	1.768 91
[¹⁸ O]-H ₂ CCO	0.0779	0.0036	0.0042	1.782 70	1.768 86
[¹⁷ O]-H ₂ CCO	0.0779	0.0038	0.0044	1.782 59	1.768 75
$[1,2^{-13}C]$ - H_2CCO	0.0766	0.0031	0.0037	1.782 95	1.769 11
$[2,2-^{2}H]-H_{2}CCO$	0.1089	0.0036	0.0042	3.561 73	1.768 40
$[2,2^{-2}H, 2^{-13}C]-H_2CCO$	0.1086	0.0036	0.0042	3.561 74	1.768 40
$[2,2^{-2}H, 1^{-13}C]-H_2CCO$	0.1086	0.0036	0.0042	3.561 74	1.768 40
[2,2- ² H, ¹⁸ O]-H ₂ CCO	0.1095	0.0036	0.0042	3.561 75	1.768 40
$[2,2-^{2}H,^{17}O]-H_{2}CCO$	0.1093	0.0037	0.0043	3.561 77	1.768 42
$[2-^{2}H]-H_{2}CCO$	0.0964	0.0037	0.0043	2.594 89	
$[2^{-2}H, 2^{-13}C]$ - H_2CCO	0.0963	0.0037	0.0043	2.598 82	
$[2^{-2}H, 1^{-13}C]$ - H_2CCO	0.0961	0.0036	0.0042	2.595 32	
[2- ² H, ¹⁸ O]-H ₂ CCO	0.0969	0.0037	0.0043	2.595 58	
$[2-^{2}H,^{17}O]-H_{2}CCO$	0.0966	0.0036	0.0042	2.595 31	
Average (\bar{x})	0.0918	0.0036	0.0042		
Std dev (s)	0.0132	0.0001	0.0001		

 $^{{}^{\}mathbf{a}}\Delta_{i} = I_{c} - I_{a} - I_{b} = -2P_{cc}.$

^bVibration-rotation interaction corrections only.

^cVibration-rotation interaction and electron-mass corrections.

 $^{^{}d}P_{bb} = (I_b - I_a - I_c)/-2.$

 $^{{}^{}e}m_{H} = 1.007 825 035 \text{ for } {}^{1}\text{H or } 2.014 101 779 \text{ for } {}^{2}\text{H}.$

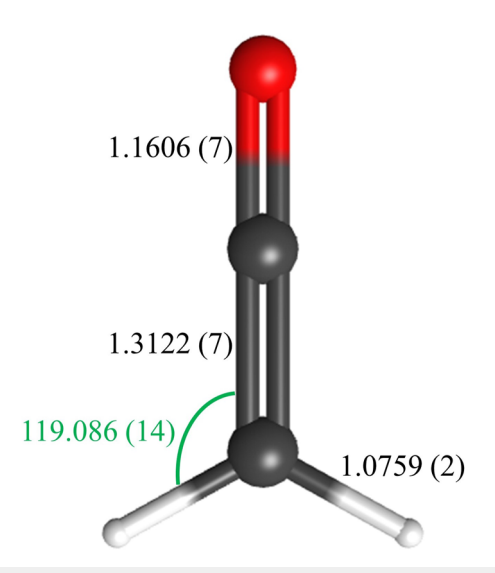


FIG. 7. Semi-experimental equilibrium structure ($r_{\rm e}^{\rm SE}$) of ketene with 2σ statistical uncertainties from least-squares fitting of the moments of inertia from 16 isotopologues. Distances are in angstroms, and the angle is in degrees.

uncertainties of heavy-atom bond lengths are nearly identical for HN₃ and ketene (0.000 74 for N1-N2; 0.000 75 for N2-N3; and 0.000 69 for C1-C2; 0.000 66 for C1-O). The 2σ statistical uncertainty for the respective X-H bond is also quite similar (0.0003 for HN₃ and 0.0002 for ketene). More generally, the bond length accuracy of the $r_e^{\rm SE}$ of ketene is similar to our other works, including heterocyclic 32,111 and is of the same order of magnitude for the accuracy in the angles, with that in ketene being more accurately determined. This improvement in accuracy is largely due to having 8× more independent moments of inertia than structural parameters (three bond lengths and one angle) for ketene. Table IV presents the $r_e^{\rm SE}$ structural parameters determined in the complete analysis, as well as the recommended $r_e^{\rm SE}$ structural parameters, which take into account the limits of precision in their determination. The distinction between these sets of values is discussed in greater detail in the next section.

DISCUSSION

In accordance with previous structure determinations, 80-85 the effect of including the available isotopologues in the $r_e^{\,\mathrm{SE}}$ structure is examined using xrefiteration.82 Figure 8 shows a plot of parameter uncertainty as a function of the number of incorporated isotopologues and reveals that the total uncertainty and the uncertainty of both the bond distances and bond angle have converged with the inclusion of the 11th isotopologue. Coincidentally, this is the same number of isotopologues used in the $r_e^{\rm SE}$ determination published by Guarnieri et al.58 The composition of the set of 11 isotopologues, however, is different in each case. Guarnieri et al. 50 determined the r_e^{SE} with mainly protio- and [2,2- 2 H]-ketene isotopologues, while the first 11 isotopologues utilized by xrefiteration in the current work include a mix of protio-, [2-2H]-ketene, and [2,2-2H]-ketene isotopologues. The addition of the five other isotopologues beyond the 11th neither decreases nor increases the total uncertainty, which is similar to the situation observed with HN₃⁸³ but unlike the cases of thiophene⁸⁰ and 1H- and 2H-1,2,3-triazole,⁸⁵ where the statistical uncertainty increases with the inclusion of the final isotopologues. Figure 9 shows the structural parameter values and their uncertainties as a function of the number of ketene isotopologues, added in the same order as in Fig. 8. It is evident that the structural parameters are well-determined with the core set of isotopologues because they agree with the respective BTE values. The addition of further isotopologues, however, decreases the 2σ uncertainties for all parameters until the addition of the 11th isotopologue, similar to Fig. 8. The r_{C-C} and r_{C-O} bond lengths of the current $r_e^{\rm SE}$ are both smaller than the respective BTE values (by 0.0003 and 0.0004 Å, respectively), while there is quite close agreement between the $r_{\rm C-H}$ bond lengths ($r_{\rm eC-H} - r_{\rm e}^{\rm SE}_{\rm C-H} = 0.000\,04$ Å). The value of the bond angle, θ_{C-C-H} , is slightly larger (0.009°) than the BTE value. Both heavy-atom bond distances of the r_e BTE structure are too large (Fig. 9) relative to their r_e^{SE} parameters, and the observed residuals are very similar to those we observed in HN₃, 83 0.000 35 Å for the central $r_{\text{N1-N2}}$ bond and 0.000 41 Å for the terminal RN2-N3 bond. In the structural least-squares fitting from rotational constants, the most difficult atom to locate is the heavy atom nearest to the center of mass, but an error in its location would tend to make one heavy-atom distance too long and one too short, contrary to the observations in ketene and HN3. This may suggest that these residual discrepancies, which are not present in the distances involving H

TABLE IV. Equilibrium structural parameters of ketene. Boldface indicates recommended values.

	$r_e^{\rm SEa,b}$ East et al. ⁵⁷	$r_e^{\rm SEa,c}$ Guarnieri <i>et al.</i> ⁵⁸	$r_e^{\rm SE}$ this work	$r_e^{\rm SE}$ recommended	CCSD(T) BTE	CCSD(T)/cc-pCV6Z
r _{C-C} (Å)	1.312 12 (60)	1.3122 (12)	1.312 18 (69)	1.3122 (7)	1.312 58	1.312 00
$r_{\text{C-H}}$ (Å)	1.075 76 (14)	1.0763 (2)	1.075 93 (16)	1.0759 (2)	1.075 89	1.075 65
$r_{\text{C-O}}$ (Å)	1.160 30 (58)	1.1607 (12)	1.160 64 (66)	1.1606 (7)	1.160 97	1.160 07
$\theta_{\text{C-C-H}}$ (deg)	119.110 (12)	119.115 (22)	119.086 (14)	119.086 (14)	119.077	119.067
$N_{ m iso}{}^{ m d}$	6	11	16	16		

^a2σ uncertainties calculated based on the uncertainty presented in each work.

^bVibration-rotation corrections calculated at a mixed MP2 and CCSD(T) level.

^cVibration-rotation and electron-mass corrections calculated at the MP2/cc-pVTZ level.

^dNumber of isotopologues used in the structure determination.

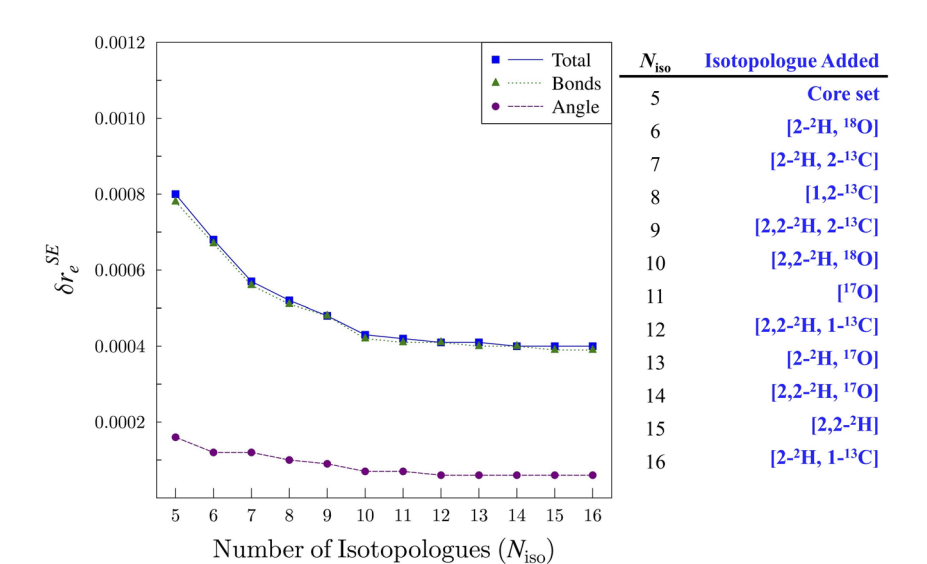
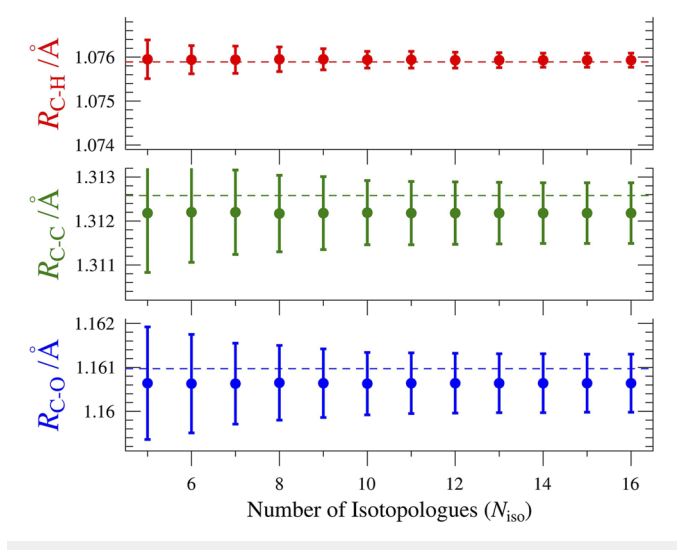


FIG. 8. Plot of r_e^{SE} uncertainty (δr_e^{SE}) as a function of the number of isotopologues (N_{iso}) incorporated into the structure determination dataset for ketene. The total relative statistical uncertainty (δr_e^{SE}) , blue squares), the relative statistical uncertainty in the bond distances (green triangles), and the relative statistical uncertainty in the angle (purple circles) are presented.

atoms, are due to some systematic shift in the BTE distances related to the heavy atom backbone of these molecules.

A graphical representation of all the structural parameters for the current r_e^{SE} , the r_e^{SE} by East et al.,⁵⁷ the r_e^{SE} by Guarnieri et al.,58 the BTE, and various coupled-cluster calculations with different basis sets is shown in Fig. 10. Upon cursory inspection, it seems there is excellent agreement among all of the structural parameters of the three r_e^{SE} structures (Table IV and Fig. 10), and all are quoted to similar precision. Because separate sets of discrepancies are involved with respect to the two previous r_e^{SE} structure determinations, we will discuss them separately. The heavy-atom distances from Guarnieri et al.⁵⁸ are essentially the same as our own, although

with slightly larger 2σ uncertainties due to the smaller dataset compared to the present work, and BTE results for both parameters easily fall within the quoted 2σ limit. The agreement for the two parameters involving the hydrogen-atom position is not quite as good. The $r_{\text{C-H}}$ bond distance from Guarnieri et al. is in disagreement with our value by slightly more than the combined 2σ error estimates, and the BTE value falls well outside their $2\sigma\,error\,range.$ The angle, $\theta_{\text{C-C-H}}$, is, indeed, in agreement with our value within the combined estimated 2σ error limits, but the BTE value of this parameter falls significantly outside their 2σ error range. We believe that the reason for these discrepancies is the impact of untreated coupling between vibrational states impacting the rotational constants. It is



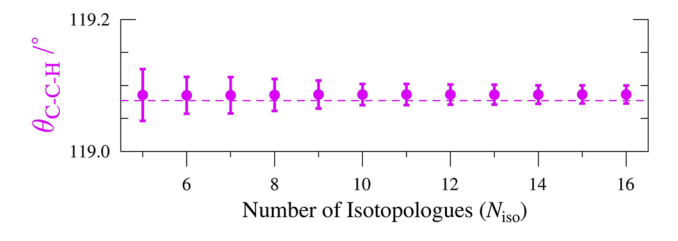


FIG. 9. Plots of the structural parameters of ketene as a function of the number of isotopologues ($N_{\rm iso}$) and their 2σ uncertainties. Plots of bond distance use consistent scales. The colored dashed lines indicate the BTE value. The table in Fig. 8 indicates the xth isotopologue added to the r_e SE

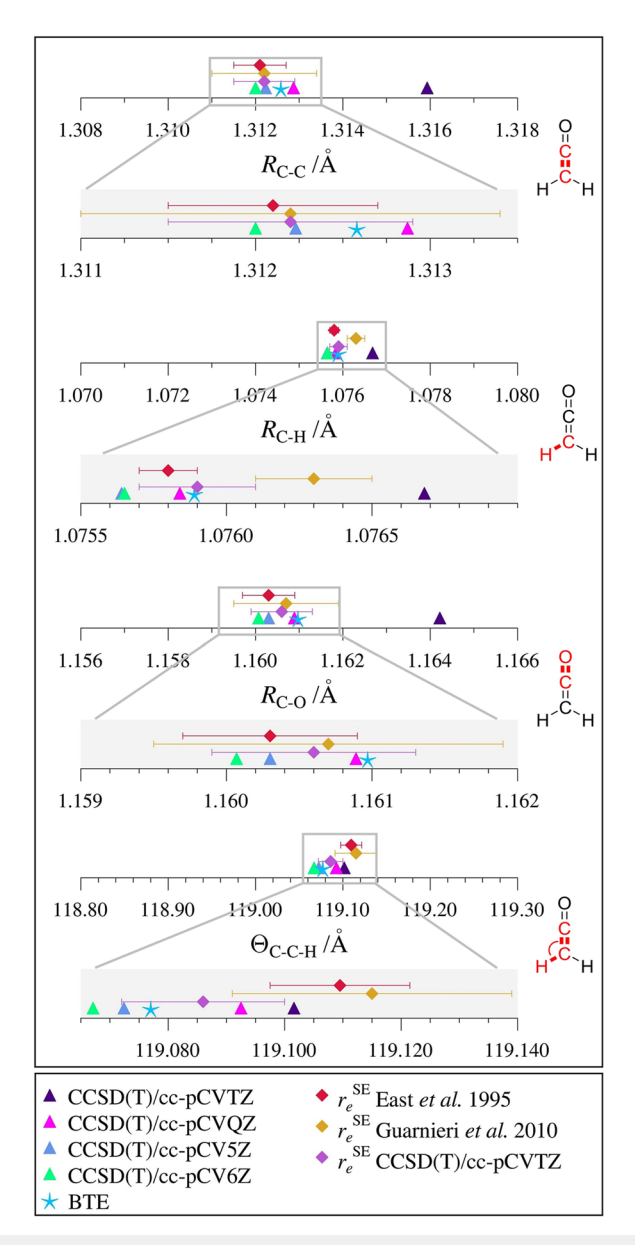


FIG. 10. Graphical comparison of the ketene structural parameters with bond distances in angstroms (Å) and angles in degrees (°). Plots of bond distance use the same scale. Expansions are provided for each parameter in gray boxes. The statistical uncertainties for all $r_{\rm e}^{\rm SE}$ parameters are 2σ .

known that the ground state of ketene at high K_a values is affected by perturbations from low-lying vibrational states. We have chosen to employ only measurements for $K_a = 0$ –5, which removed this problem. Guarnieri *et al.*, ⁵⁸ however, used higher K_a transitions in their least-squares fits, which required the inclusion of higher-order centrifugal distortion terms, L_{JK} and L_{JKK} . These effective parameters distort the determined values of A_0 from the regression analysis, which may affect the structural parameters. We tested our conjecture by using our rotational constants for the set of isotopologues

used by Guarnieri *et al.*⁵⁸ and found the resultant structure in essentially complete agreement with our own $r_e^{\rm SE}$ structure (Table IV), which is consistent with the analysis of the structure shown in Fig. 9. This indicates that the five additional isotopologues that we measured and included were not required to achieve this improved accuracy.

The situation with respect to the r_e^{SE} structure from East *et al.*⁵⁷ is more straightforward. The bond distances and angles reported by East et al. 57 are in complete agreement with the current $r_e^{\rm SE}$ values. This is somewhat surprising, given that the rotational constants are substantially less precise than the values determined in the present work and that the A_0 constant of [¹⁸O]-ketene used by East et al.⁵⁷ and determined experimentally by Brown et al.,²⁸ 287 350 (910) MHz, is clearly too large by about 5 GHz. The values of A_0 for all heavy-atom isotopologues should be nearly the same because they depend only on the distance of the hydrogen atoms from the a-axis. This is confirmed by the data in Table II. The remaining rotational constants used by East et al.57 are all similar to those in the present work. We obtained an r_e^{SE} structure using the rotational constants and vibration-rotation interaction corrections presented in Table XIV of the East et al.⁵⁷ work and obtained a structure very closely resembling the one presented in that work for all parameters. This is also an interesting outcome, as the vibration-rotation interaction corrections used in that work are clearly inadequate, as evidenced by the residual inertial defects presented in their Table XIV⁵⁷ that vary in sign and order of magnitude across the six isotopologues. Despite the inadequacy of the vibration-rotation interaction corrections, the $r_e^{\rm SE}$ structure of East et al.⁵⁷ is in excellent agreement with the new $r_e^{\rm SE}$ but not quite in agreement with the $heta_{
m C-C-H}$ value from the r_e BTE structure. These analyses are provided in the supplementary material and summarized in Tables S-V and S-VI.

The r_e^{SE} structure presented in this work, like the previously reported structures,⁵ suffers from the impact of untreated Coriolis coupling between its ground state and its vibrationally excited states. Despite this limitation, the 2σ statistical uncertainties for the bond distances and bond angles are quite small (0.0002 to 0.0007 Å for the bond distances and 0.014° for the bond angle). For the bond distances, this statistical uncertainty is approaching the limit of the r_e^{SE} structure determination, which requires the assumption that there is one mass-independent equilibrium geometry. The mass independence of equilibrium structures is a tacitly accepted assumption of molecular structure determination by rotational spectroscopy that is no longer valid as the limits of accuracy and precision are extended, especially for parameters involving hydrogen atoms. As a simple test of this assumption, optimized geometries were obtained for ketene and [2,2-2H]-ketene with and without the diagonal Born-Oppenheimer correction (DBOC; SCF with the aug-cc-pCVTZ basis set). Of course, the r_e structure obtained from the normal optimization without the DBOC resulted in the same equilibrium geometry for both isotopologues. With the DBOC, however, the equilibrium C-D distance decreased relative to the C-H distance by 0.000 06 Å. This value, which is similar to that obtained for benzene,86 suggests that the limit and trustworthiness of the r_e^{SE} structure for ketene and other C-H containing $r_e^{\rm SE}$ structures is on the order of 0.0001 Å, which is half of the 2σ statistical uncertainty of the r_e^{SE} C-H distance in this work. As a consequence of these relationships, our recommended values for the structural parameters of ketene are $r_{C-C} = 1.3122$ (7) Å,

 $r_{\text{C-H}} = 1.0759$ (2) Å, $r_{\text{C-O}} = 1.1606$ (7) Å, and $\theta_{\text{C-C-H}} = 119.086$ (14)°, as shown in Fig. 7 and Table IV.

The $C_{2\nu}$ symmetry of ketene- h_2 and ketene- d_2 allows for two independent confirmations of the quality of the spectroscopic analysis and computational corrections, P_{bb} and Δ_{ie} . Δ_{ie} for a planar molecule is zero, as no nuclear mass exists off of the molecular plane. Any residual inertial defect after correction of the rotational constants for the vibration-rotation interaction and the electronic mass distribution potentially reveals room for improvements in the rotational constants or computational corrections. While all of the residual Δ_{ie} values are quite small (Table III), their non-zero values demonstrate that further corrections may be possible. Their scatter reveals an interesting mass dependence. The ketene- d_1 and ketene d_2 isotopologues have nearly identical inertial defects to four decimal places (0.0042 or 0.0043 μ Å²), while the ketene- h_2 isotopologues have an average value of $(0.0042 \ \mu\text{Å}^2)$ and a range from 0.0037 to $0.0044 \,\mu\text{Å}^2$. To probe this mass dependence, we determined the P_{bb} (second moments) value¹¹² for each isotopologue (Table III), after computational corrections were applied to the rotational constants. To the extent that there is a single, mass-independent equilibrium geometry of ketene, the P_{bb} value, corrected for the mass of the hydrogen or deuterium atom in the $C_{2\nu}$ isotopologues (ketene- h_2 and ketene- d_2), should be the same for all isotopologues because it is only dependent on the location of the H atoms with respect to the perpendicular mirror plane. Also shown in Table III are the P_{bb}/m_H values, which are practically identical for all of the ketene- d_2 isotopologues (1.7684 Å²). The P_{bb}/m_H values for the protio-ketene isotopologues show an increased scatter ranging from 1.7687 to 1.7691 Å^2 but have a higher average value as well (1.7689 Å²). While these differences are small, their clear mass dependence leads us to conclude that we have not completely removed the impact of untreated Coriolis coupling from the rotational constants. The larger mass of ${}^{2}H$ compared to ${}^{1}H$ reduces the A_{0} rotational constant by roughly a factor of two for the deuterium-containing isotopologues. The a-axis Coriolis ζ is unchanged between isotopologues, but the a-axis Coriolis coupling constants scale with the magnitude of the A_0 rotational constant. It is expected, therefore, that the protioketenes would be subject to a slightly greater impact of untreated Coriolis coupling, which is consistent with this observation. The great constancy of the $P_{\rm bb}/m_{\rm D}$ values across all the [2,2- 2 H]-ketene isotopologues (vide supra) leads us to believe that the corresponding b-coordinate of the ²H-atom [0.940 32 Å, determined by Eq. (3)] is one of the most reliably determined structural parameters of ketene,

$$b_H = \sqrt{\frac{P_{bb}}{2m_H}}. (3)$$

This assertion is supported by a comparison to its corresponding values calculated from the internal coordinates in Table IV: $r_e^{\rm SE}=0.940$ 25 Å, r_e 6Z = 0.940 17 Å, and r_e BTE = 0.940 29 Å. The very small difference from the BTE value (0.000 03 Å) is particularly notable and satisfying. The corresponding value for the b-coordinate of the 1 H-atom in ketene is 0.940 45 Å, which is slightly larger due to some combination of the true isotopic difference in the $r_{\rm C-H}$ and $r_{\rm C-D}$ equilibrium bond distances and the increased untreated Coriolis coupling in the protio-ketene isotopologues.

CONCLUSION

A new, highly precise, and accurate semi-experimental equilibrium (r_e^{SE}) structure for ketene (H₂C=C=O) has been determined from the rotational spectra of 16 isotopologues. The 2σ values for the r_e^{SE} structure of ketene, and also the discrepancies between the best theoretical estimate (BTE) and the r_e^{SE} structural parameters, are strikingly similar to those for the previous r_e^{SE} structure of hydrazoic acid (HNNN).83 This outcome is noteworthy, although perhaps not surprising, given (i) the structural similarity between the two species and (ii) the highly over-determined datasets, which are a consequence of the large number of isotopologues relative to the number of structural parameters. In both cases, we found that extrapolation to the complete basis set limit provided slightly better agreement with the $r_e^{\rm SE}$ structure when the highest level calculation included in the extrapolation was CCSD(T)/cc-pCV6Z, as opposed to CCSD(T)/cc-pCV5Z. It is somewhat surprising that the high accuracy of the ketene structure did not require the full dataset from 16 isotopologues. The uncertainties in the structural parameters did not improve with the inclusion of the "last" five isotopologues in the *xrefiteration* analysis. This case stands in contrast to other molecules that we have studied, in which quite large numbers of isotopologues are required for convergence of the $r_e^{\rm SE}$ parameters. Review Previous Previous Review Previous Rev ous studies were steering us toward a generalization that "more is better" with respect to the number of isotopologues used in a structure determination, but the current case provides a counterexample. In the current case, the extra isotopologues do not degrade the quality of the structure, but they do not improve it. The current state of understanding of r_e^{SE} structure determination does not enable a prediction of the number of isotopologues that will be required for the statistical uncertainties of the structural parameters to converge.

The present work confirms the great utility of the BTE structure as a benchmark for the semi-experimental structures. Although both of the published $r_e^{\rm SE}$ structures for ketene, to which we have compared our own results, are generally in excellent agreement with the present work, the comparison to the BTE structure clearly establishes that the present approach of limiting the dataset to low K_a values (0–5) improved the results for a molecule in which perturbations of the ground state exist. There need to be further investigations of why the BTE structure predicts heavy-atom bond distances that are longer than the $r_e^{\rm SE}$ structure when all of the other structural parameters agree so well. The BTE values for the heavy-atom distances do not fall outside the 2σ statistical uncertainty of the $r_e^{\rm SE}$ values, but the small differences between BTE and $r_e^{\rm SE}$ values have now been observed in both ketene and HN₃. The general applicability to similar molecules and the origin of the effect merit additional study.

The current studies enhance the capability for radioastronomers to search for ketene in different extraterrestrial environments by extending the measured frequency range of ketene to 750 GHz as well as providing data for newly measured isotopologues, [2-²H, 1-¹³C]-ketene, [2-²H, 2-¹³C]-ketene, [2-²H, ¹⁸O]-ketene, [2-²H, ¹⁷O]-ketene, and [2,2-²H, ¹⁷O]-ketene. These new data will also be valuable for identifying these species in laboratory experiments, e.g., electric discharge, pyrolysis, and photolysis. Finally, these spectra contain a great many transitions from vibrationally excited states, which should prove valuable in analyzing and quantifying the numerous perturbations that exist between these

low-lying vibrational states. We hope to pursue this topic in the future.

SUPPLEMENTARY MATERIAL

Computational output files, least-squares fitting for all isotopologues, data distribution plots for all non-standard isotopologues, *xrefiteration* outputs, equations used for calculating determinable constants and BTE corrections, and tables of S-reduction, A-reduction, and determinable constants, structural parameters, inertial defects, BTE corrections, and synthetic details are provided in the supplementary material.

ACKNOWLEDGMENTS

We gratefully acknowledge the funding from the U.S. National Science Foundation for the support of this project (Grant No. CHE-1954270 to R.J.M and Grant No. CHE-1664325 to J.F.S.). We thank Maria Zdanovskaia for her assistance with generating figures. We thank Maria Zdanovskaia and Andrew Owen for their thoughtful commentary and review of the manuscript. We thank Tracy Drier for the construction of the ketene lamp used in this work.

AUTHOR DECLARATIONS

Conflict of Interest

The authors have no conflicts to disclose.

Author Contributions

Houston H. Smith: Formal analysis (equal); Investigation (equal); Writing – original draft (equal); Writing – review & editing (equal). Brian J. Esselman: Conceptualization (equal); Formal analysis (equal); Investigation (equal); Supervision (equal); Writing – original draft (equal); Writing – review & editing (equal). Samuel A. Wood: Investigation (equal); Methodology (equal); Writing – review & editing (equal). John F. Stanton: Formal analysis (equal); Investigation (equal); Software (equal); Writing – review & editing (equal). R. Claude Woods: Conceptualization (equal); Formal analysis (equal); Investigation (equal); Supervision (equal); Writing – review & editing (equal). Robert J. McMahon: Funding acquisition (lead); Investigation (equal); Project administration (equal); Supervision (equal); Writing – review & editing (equal).

DATA AVAILABILITY

The data that support the findings of this study are available within the article and its supplementary material.

REFERENCES

- ¹T. T. Tidwell, Ketenes, 2nd ed. (John Wiley & Sons, Hoboken, NJ, 2006).
- ²R. L. Danheiser, Science of Synthesis: Three Carbon-Heteroatom Bonds: Ketenes and Derivatives (Georg Thieme Verlag, Stuttgart, 2006), Vol. 23.
- ³ A. D. Allen and T. T. Tidwell, "New directions in ketene chemistry: The land of opportunity," Eur. J. Org. Chem. **2012**, 1081–1096.
- ⁴Y. Zhang, P. Gao, F. Jiao, Y. Chen, Y. Ding, G. Hou, X. Pan, and X. Bao, "Chemistry of ketene transformation to gasoline catalyzed by H-SAPO-11," J. Am. Chem. Soc. **144** 18251–18258 (2022).

- ⁵F. A. Leibfarth and C. J. Hawker, "The emerging utility of ketenes in polymer chemistry," J. Polym. Sci., Part A: Polym. Chem. **51**, 3769–3782 (2013).
- ⁶M. J. Newland, G. J. Rea, L. P. Thüner, A. P. Henderson, B. T. Golding, A. R. Rickard, I. Barnes, and J. Wenger, "Photochemistry of 2-butenedial and 4-oxo-2-pentenal under atmospheric boundary layer conditions," Phys. Chem. Chem. Phys. 21, 1160 (2019).
- ⁷W. Sun, J. Wang, C. Huang, N. Hansen, and B. Yang, "Providing effective constraints for developing ketene combustion mechanisms: A detailed kinetic investigation of diacetyl flames," Combust. Flame 205, 11–21 (2019).
- ⁸R. L. Hudson and M. J. Loeffler, "Ketene formation in interstellar ices: A laboratory study," Astrophys. J. 773, 109 (2013).
- ⁹B. E. Turner, "Microwave detection of interstellar ketene," Astrophys. J. **213**, L75–L79 (1977).
- ¹⁰H. E. Matthews and T. J. Sears, "Interstellar molecular line searches at 1.5 centimeters," Astrophys. J. 300, 766–772 (1986).
- ¹¹L. E. B. Johansson, C. Andersson, J. Ellder, P. Friberg, A. Hjalmarson, B. Hoglund, W. M. Irvine, H. Olofsson, and G. Rydbeck, "Spectral scan of Orion A and IRC+10216 from 72 to 91 GHz," Astron. Astrophys. 130, 227–256 (1984).
 ¹²W. M. Irvine, P. Friberg, N. Kaifu, K. Kawaguchi, Y. Kitamura, H. E. Matthews, Y. Minh, S. Saito, N. Ukita, and S. Yamamoto, "Observations of some oxygen-containing and sulfur-containing organic molecules in cold dark clouds," Astrophys. J. 342, 871–875 (1989).
- ¹³B. E. Turner, R. Terzieva, and E. Herbst, "The physics and chemistry of small translucent molecular clouds. XII. More complex species explainable by gas-phase processes," Astrophys. J. **518**, 699–732 (1999).
- ¹⁴ A. Bacmann, V. Taquet, A. Faure, C. Kahane, and C. Ceccarelli, "Detection of complex organic molecules in a prestellar core: A new challenge for astrochemical models," Astron. Astrophys. 541, L12 (2012).
- ¹⁵J. K. Jørgensen, H. S. P. Müller, H. Calcutt, A. Coutens, M. N. Drozdovskaya, K. I. Öberg, M. V. Persson, V. Taquet, E. F. van Dishoeck, and S. F. Wampfler, "The ALMA-PILS survey: Isotopic composition of oxygen-containing complex organic molecules toward IRAS 16293–2422B," Astron. Astrophys. 620, A170 (2018).
- ¹⁶S. Muller, A. Beelen, M. Guélin, S. Aalto, J. H. Black, F. Combes, S. J. Curran, P. Theule, and S. N. Longmore, "Molecules at z = 0.89. A 4-mm-rest-frame absorption-line survey toward PKS 1830-211," Astron. Astrophys. 535, A103 (2011).
- ¹⁷H. Staudinger, *Die Ketene* (Enke Verlag, Stuttgart, 1912).
- ¹⁸S. C. Wang and F. W. Schueler, "A simple ketene generator," J. Chem. Educ. 26, 323 (1949).
- ¹⁹G. Quadbeck, "Neuere Methoden der präparativen organischen Chemie II. Keten in der präparativen organischen Chemie," Angew. Chem. 68, 361–370 (1956).
- ²⁰ E. M. S. Maçôas, L. Khriachtchev, R. Fausto, and M. Räsänen, "Photochemistry and vibrational spectroscopy of the *trans* and *cis* conformers of acetic acid in solid Ar," J. Phys. Chem. A **108**, 3380–3389 (2004).
- ²¹ X. K. Zhang, J. M. Parnis, E. G. Lewars, and R. E. March, "FTIR spectroscopic investigation of matrix-isolated isomerization and decomposition products of ionized acetone: Generation and characterization of 1-propen-2-ol," Can. J. Chem. 75, 276–284 (1997).
- ²²B. J. Esselman and N. J. Hill, "Proper resonance depiction of Acylium cation: A high-level and student computational investigation," J. Chem. Educ. **92**, 660–663 (2015).
- ²³ J. Cernicharo, C. Cabezas, S. Bailleux, L. Margulès, R. Motiyenko, L. Zou, Y. Endo, C. Bermúdez, M. Agúndez, N. Marcelino, B. Lefloch, B. Tercero, and P. de Vicente, "Discovery of the acetyl cation, CH₃CO⁺, in space and in the laboratory," Astron. Astrophys. **646**, L7 (2021).
- ²⁴B. Bak, E. S. Knudsen, E. Madsen, and J. Rastrup-Andersen, "Preliminary analysis of the microwave spectrum of ketene," Phys. Rev. **79**, 190 (1950).
- ²⁵H. R. Johnson and M. W. P. Strandberg, "The microwave spectrum of ketene," J. Chem. Phys. **20**, 687–695 (1952).
- ²⁶ A. P. Cox, L. F. Thomas, and J. Sheridan, "Internuclear distances in keten from spectroscopic measurements," Spectrochim. Acta 15, 542–543 (1959).
- ²⁷R. A. Beaudet, "Problems in molecular structure and internal rotation," Ph.D. dissertation (Harvard University, 1962).

- ²⁸ R. D. Brown, P. D. Godfrey, D. McNaughton, A. P. Pierlot, and W. H. Taylor, "Microwave spectrum of ketene," J. Mol. Spectrosc. **140**, 340–352 (1990).
- ²⁹V. W. Weiss and W. H. Flygare, "Hydrogen spin–spin, spin–rotation, and deuterium nuclear quadrupole interactions in ketene, ketene- d_1 , and ketene- d_2 ," J. Chem. Phys. **45**, 3475–3476 (1966).
- ³⁰L. Nemes and M. Winnewisser, "Centrifugal distortion analysis of the microwave and millimeter wave spectra of deuterated ketenes," Z. Naturforsch., A 31, 272–282 (1976).
- ³¹ A. Guarnieri and A. Huckauf, "The rotational spectrum of (¹⁷O) ketene,"
 Z. Naturforsch., A: Phys. Sci. 56, 440-446 (2001).
- ³²A. Guarnieri, "The millimeterwave spectrum of four rare ketene isotopomers," Z. Naturforsch., A: Phys. Sci. **60**, 619–628 (2005).
- 33 L. Nemes, J. Demaison, and G. Wlodarczak, "New measurements of submillimetre-wave rotational transitions for the ketene (H₂CCO) Molecule," Acta Phys. Hung. **61**, 135–138 (1987).
- ³⁴H. Gershinowitz and E. B. Wilson, "Infrared absorption spectrum of ketene," J. Chem. Phys. 5, 500 (1937).
- 35 F. Halverson and V. Z. Williams, "The infra-red spectrum of ketene," J. Chem. Phys. 15, 552–559 (1947).
- ³⁶W. R. Harp and R. S. Rasmussen, "The infra-red absorption spectrum and vibrational frequency assignment of ketene," J. Chem. Phys. **15**, 778–785 (1947).
- ³⁷L. G. Drayton and H. W. Thompson, "The infra-red spectrum of keten," J. Chem. Soc. 1948, 1416–1419.
- ³⁸B. Bak and F. A. Andersen, "The infrared spectrum of ketene," J. Chem. Phys. 22, 1050–1053 (1954).
- ³⁹P. E. B. Butler, D. R. Eatcw, and H. W. Thompson, "Vibration-rotation bands of keten," Spectrochim. Acta 13, 223–235 (1958).
- ⁴⁰W. H. Fletcher and W. F. Arendale, "Infrared spectra of CD₂CO and CHDCO," J. Chem. Phys. **19**, 1431–1432 (1951).
- ⁴¹ W. F. Arendale and W. H. Fletcher, "Some vibration-rotation bands of ketene," J. Chem. Phys. **24**, 581–587 (1956).
- ⁴²W. F. Arendale and W. H. Fletcher, "Infrared spectra of ketene and deuteroketenes," J. Chem. Phys. **26**, 793–797 (1957).
- detiteroketenes, J. Chem. Phys. 26, 793–797 (1957).

 43 A. P. Cox and A. S. Esbitt, "Fundamental vibrational frequencies in ketene and
- the deuteroketenes," J. Chem. Phys. **38**, 1636–1643 (1963).

 44 L. Nemes, "Multiple Coriolis perturbations in the vibrational-rotational spectrum of letters and diductive letters." Torior Deld. Simp. Mol. Scalebrack. Visc
- tra of ketene and dideuteroketene," Tezisy Dokl. Simp. Mol. Spektrosk. Vys. Sverkhvys. Razresheniya, 2nd; Akad. Nauk SSSR, Sib. Otd., Inst. Opt. Atmos. 2 (1974).
- ^{45}L . Nemes, "Rotation-vibration analysis of the Coriolis-coupled $\nu_5,\nu_6,\nu_8,$ and ν_9 bands of H₂CCO," J. Mol. Spectrosc. **72**, 102–123 (1978).
- ⁴⁶F. Winther, F. Hegelund, and L. Nemes, "The infrared spectrum of dideuteroketene below 620 cm⁻¹," J. Mol. Spectrosc. **117**, 388–402 (1986).
- $^{\bf 47}$ J. L. Duncan, A. M. Ferguson, J. Harper, K. H. Tonge, and F. Hegelund, "High-resolution infrared rovibrational studies of the $\rm A_1$ species fundamentals of isotopic ketenes," J. Mol. Spectrosc. 122, 72–93 (1987).
- ⁴⁸J. L. Duncan and A. M. Ferguson, "High resolution infrared analyses of fundamentals and overtones in isotopic ketenes," Spectrochim. Acta, Part A 43, 1081–1086 (1987).
- ⁴⁹F. Hegelund, J. Kauppinen, and F. Winther, "The high resolution infrared spectrum of the ν₉, ν₆ and ν₅ bands in ketene-d₂," Mol. Phys. **61**, 261–273 (1987).
- 50 R. Escribano, J. L. Doménech, P. Cancio, J. Ortigoso, J. Santos, and D. Bermejo, "The ν_1 band of ketene," J. Chem. Phys. $\bf 101$, 937–949 (1994).
- 51 M. C. Campiña, E. Domingo, M. P. Fernández-Liencres, R. Escribano, and L. Nemes, "Analysis of the high resolution spectra of the ν_5 and ν_6 bands of ketene," An. Quim., Int. Ed. $\bf 94$, 23–26 (1998)..
- 52 M. Gruebele, J. W. C. Johns, and L. Nemes, "Observation of the $\nu_6 + \nu_9$ band of ketene via resonant Coriolis interaction with ν_8 ," J. Mol. Spectrosc. **198**, 376–380 (1999).
- ⁵³ J. W. C. Johns, L. Nemes, K. M. T. Yamada, T. Y. Wang, J. Doménech, J. Santos, P. Cancio, D. Bermejo, J. Ortigoso, and R. Escribano, "The ground state constants of ketene," J. Mol. Spectrosc. 156, 501–503 (1992).
- ⁵⁴L. Nemes, D. Luckhaus, M. Quack, and J. W. C. Johns, "Deperturbation of the low-frequency infrared modes of ketene (CH₂CO)," J. Mol. Struct. **517-518**, 217-226 (2000).

- 55 P. D. Mallinson and L. Nemes, "The force field and r_z structure of ketene," J. Mol. Spectrosc. 59, 470–481 (1976).
- ⁵⁶J. L. Duncan and B. Munro, "The ground state average structure of ketene," J. Mol. Struct. **161**, 311–319 (1987).
- ⁵⁷ A. L. L. East, W. D. Allen, and S. J. Klippenstein, "The anharmonic force field and equilibrium molecular structure of ketene," J. Chem. Phys. **102**, 8506–8532 (1995)
- ⁵⁸ A. Guarnieri, J. Demaison, and H. D. Rudolph, "Structure of ketene—Revisited r_e (equilibrium) and r_m (mass-dependent) structures," J. Mol. Struct. **969**, 1–8 (2010).
- ⁵⁹ J. L. Duncan, A. M. Ferguson, J. Harper, and K. H. Tonge, "A combined empirical-ab initio determination of the general harmonic force field of ketene," J. Mol. Spectrosc. 125, 196–213 (1987).
- ⁶⁰ A. Guarnieri and A. Huckauf, "The rotational spectrum of ketene isotopomers with ¹⁸O and ¹³C revisited," Z. Naturforsch., A: Phys. Sci. **58**, 275–279 (2003).
- ⁶¹C. C. Costain, "Determination of molecular structures from ground state rotational constants," J. Chem. Phys. 29, 864–874 (1958).
- ⁶² M. D. Harmony, V. W. Laurie, R. L. Kuczkowski, R. H. Schwendeman, D. A. Ramsay, F. J. Lovas, W. J. Lafferty, and A. G. Maki, "Molecular structures of gas-phase polyatomic molecules determined by spectroscopic methods," J. Phys. Chem. Ref. Data 8, 619–722 (1979).
- ⁶³ P. Pulay, W. Meyer, and J. E. Boggs, "Cubic force constants and equilibrium geometry of methane from Hartree–Fock and correlated wavefunctions," J. Chem. Phys. 68, 5077–5085 (1978).
- ⁶⁴J. Demaison, "Experimental, semi-experimental and *ab initio* equilibrium structures," Mol. Phys. **105**, 3109–3138 (2007).
- ⁶⁵J. Vázquez and J. F. Stanton, in *Equilibrium Molecular Structures: From Spectroscopy to Quantum Chemistry*, edited by J. Demaison, J. E. Boggs, and A. G. Császár (Taylor & Francis Group; CRC Press, 2010), pp 53–87.
- ⁶⁶M. Mendolicchio, E. Penocchio, D. Licari, N. Tasinato, and V. Barone, "Development and implementation of advanced fitting methods for the calculation of accurate molecular structures," J. Chem. Theory Comput. **13**, 3060–3075 (2017).
- ⁶⁷C. Puzzarini and V. Barone, "Diving for accurate structures in the ocean of molecular systems with the help of spectroscopy and quantum chemistry," Acc. Chem. Res. **51**, 548–556 (2018).
- ⁶⁸ K. Raghavachari, G. W. Trucks, J. A. Pople, and M. Head-Gordon, "A fifth-order perturbation comparison of electron correlation theories," Chem. Phys. Lett. 157, 479–483 (1989).
- ⁶⁹ J. M. L. Martin and P. R. Taylor, "The geometry, vibrational frequencies, and total atomization energy of ethylene. A calibration study," Chem. Phys. Lett. **248**, 336–344 (1996).
- ⁷⁰T. Helgaker, J. Gauss, P. Jørgensen, and J. Olsen, "The prediction of molecular equilibrium structures by the standard electronic wave functions," J. Chem. Phys. 106, 6430–6440 (1997).
- 71 K. A. Peterson and T. H. Dunning, Jr., "Benchmark calculations with correlated molecular wave functions. VIII. Bond energies and equilibrium geometries of the CH_n and C₂H_n (n=1–4) series," J. Chem. Phys. **106**, 4119–4140 (1997).
- ⁷²T. Helgaker, P. Jørgensen, and J. Olsen, *Molecular Electronic-Structure Theory* (John Wiley & Sons, 2000).
- ⁷³ K. L. Bak, J. Gauss, P. Jørgensen, J. Olsen, T. Helgaker, and J. F. Stanton, "The accurate determination of molecular equilibrium structures," J. Chem. Phys. 114, 6548–6556 (2001).
- ⁷⁴S. Coriani, D. Marchesan, J. Gauss, C. Hättig, T. Helgaker, and P. Jørgensen, "The accuracy of *ab initio* molecular geometries for systems containing second-row atoms," J. Chem. Phys. **123**, 184107 (2005).
- ⁷⁵C. Puzzarini, "Accurate molecular structures of small- and medium-sized molecules," Int. J. Quantum Chem. 116, 1513–1519 (2016).
- ⁷⁶C. Puzzarini and J. F. Stanton, "Connections between the accuracy of rotational constants and equilibrium molecular structures," Phys. Chem. Chem. Phys. 25, 1421–1429 (2023).
- ⁷⁷J. Gauss and J. F. Stanton, "Equilibrium structure of LiCCH," Int. J. Quantum Chem. 77, 305–310 (2000).
- ⁷⁸M. Piccardo, E. Penocchio, C. Puzzarini, M. Biczysko, and V. Barone, "Semi-experimental equilibrium structure determinations by employing B3LYP/SNSD

- anharmonic force fields: Validation and application to semirigid organic molecules," J. Phys. Chem. A 119, 2058–2082 (2015).
- ⁷⁹Z. N. Heim, B. K. Amberger, B. J. Esselman, J. F. Stanton, R. C. Woods, and R. J. McMahon, "Molecular structure determination: Equilibrium structure of pyrimidine (m-C₄H₄N₂) from rotational spectroscopy (r_e ^{SE}) and high-level *ab initio* calculation (r_e) agree within the uncertainty of experimental measurement," J. Chem. Phys. **152**, 104303 (2020).
- ⁸⁰ V. L. Orr, Y. Ichikawa, A. R. Patel, S. M. Kougias, K. Kobayashi, J. F. Stanton, B. J. Esselman, R. C. Woods, and R. J. McMahon, "Precise equilibrium structure determination of thiophene (*c*-C₄H₄S) by rotational spectroscopy—Structure of a five-membered heterocycle containing a third-row atom," J. Chem. Phys. **154**, 244310 (2021).
- ⁸¹B. J. Esselman, M. A. Zdanovskaia, A. N. Owen, J. F. Stanton, R. C. Woods, and R. J. McMahon, "Precise equilibrium structure of thiazole (*c*-C₃H₃NS) from twenty-four isotopologues," J. Chem. Phys. **155**, 054302 (2021).
- 82 A. N. Owen, M. A. Zdanovskaia, B. J. Esselman, J. F. Stanton, R. C. Woods, and R. J. McMahon, "Semi-experimental equilibrium $(r_e{}^{\rm SE})$ and theoretical structures of pyridazine $(o\text{-}{\rm C}_4{\rm H}_4{\rm N}_2)$," J. Phys. Chem. A 125, 7976–7987 (2021).
- 83 A. N. Owen, N. P. Sahoo, B. J. Esselman, J. F. Stanton, R. C. Woods, and R. J. McMahon, "Semi-experimental equilibrium ($r_e^{\rm SE}$) and theoretical structures of hydrazoic acid (HN₃)," J. Chem. Phys. **157**, 034303 (2022).
- ⁸⁴ H. A. Bunn, B. J. Esselman, P. R. Franke, S. M. Kougias, R. J. McMahon, J. F. Stanton, S. L. Widicus Weaver, and R. C. Woods, "Millimeter/Submillimeter-wave spectroscopy and the semi-experimental equilibrium (r_e ^{SE}) structure of 1H-1,2,4-Triazole (c- C_2 H₃N₃)," J. Phys. Chem. A **126**, 8196–8210 (2022).
- 85 M. A. Zdanovskaia, B. J. Esselman, S. M. Kougias, B. K. Amberger, J. F. Stanton, R. C. Woods, and R. J. McMahon, "Precise equilibrium structures of 1*H* and 2*H*-1,2,3-triazoles ($C_2H_3N_3$) by millimeter-wave spectroscopy," J. Chem. Phys. 157, 084305 (2022).
- ⁸⁶B. J. Esselman, M. A. Zdanovskaia, A. N. Owen, J. F. Stanton, R. C. Woods, and R. J. McMahon, "Precise equilibrium structure of benzene" (unpublished) (2023).
- ⁸⁷B. K. Amberger, B. J. Esselman, J. F. Stanton, R. C. Woods, and R. J. McMahon, "Precise equilibrium structure determination of hydrazoic acid (HN₃) by millimeter-wave Spectroscopy," J. Chem. Phys. **143**, 104310 (2015).
- ⁸⁸B. J. Esselman, B. K. Amberger, J. D. Shutter, M. A. Daane, J. F. Stanton, R. C. Woods, and R. J. McMahon, "Rotational spectroscopy of pyridazine and its isotopologs from 235–360 GHz: Equilibrium structure and vibrational satellites," J. Chem. Phys. 139, 224304 (2013).
- ⁸⁹M. A. Zdanovskaia, B. J. Esselman, R. C. Woods, and R. J. McMahon, "The 130–370 GHz rotational spectrum of phenyl isocyanide (C₆H₅NC)," J. Chem. Phys. **151**, 024301 (2019).
- ⁹⁰ H. M. Pickett, "Determination of collisional linewidths and shifts by a convolution method," Appl. Opt. 19, 2745–2749 (1980).
- ⁹¹ Z. Kisiel, L. Pszczółkowski, B. J. Drouin, C. S. Brauer, S. Yu, J. C. Pearson, I. R. Medvedev, S. Fortman, and C. Neese, "Broadband rotational spectroscopy of acrylonitrile: Vibrational energies from perturbations," J. Mol. Spectrosc. 280, 134–144 (2012).
- ⁹²Z. Kisiel, L. Pszczółkowski, I. R. Medvedev, M. Winnewisser, F. C. De Lucia, and E. Herbst, "Rotational spectrum of *trans-trans* diethyl ether in the ground and three excited vibrational states," J. Mol. Spectrosc. 233, 231–243 (2005).
- 93 H. M. Pickett, "The fitting and prediction of vibration-rotation spectra with spin interactions," J. Mol. Spectrosc. 148, 371–377 (1991).
- ⁹⁴Z. Kisiel, "Assignment and analysis of complex rotational spectra," in *Spectroscopy from Space*, edited by J. Demaison, K. Sarka, and E. A. Cohen, 1st ed. (Springer Netherlands, Dordrecht, 2001), pp 91–106.

- 95 See http://info.ifpan.edu.pl/~kisiel/prospe.htm for PROSPE—Programs for ROtational SPEctroscopy.
- 96 J. F. Stanton, J. Gauss, M. E. Harding, and P. G. Szalay, with contributions from A. A. Auer, R. J. Bartlett, U. Benedikt, C. Berger, D. E. Bernholdt, Y. J. Bomble, L. Cheng, O. Christiansen, M. Heckert, O. Heun, C. Huber, T.-C. Jagau, D. Jonsson, J. Jusélius, K. Klein, W. J. Lauderdale, D. A. Matthews, T. Metzroth, L. A. Mück, D. P. O'Neill, D. R. Price, E. Prochnow, C. Puzzarini, K. Ruud, F. Schiffmann, W. Schwalbach, S. Stopkowicz, A. Tajti, J. Vázquez, F. Wang, J. D. Watts, and the integral packages MOLECULE (J. Almlöf and P. R. Taylor), PROPS (P. R. Taylor), ABACUS (T. Helgaker, H. J. Aa. Jensen, P. Jørgensen, and J. Olsen), and ECP routines by A. V. Mitin and C. van Wüllen, CFOUR, Coupled-Cluster techniques for Computational Chemistry, a quantum-chemical program package. For the current version, see http://www.cfour.de.
- ⁹⁷ J. F. Stanton, C. L. Lopreore, and J. Gauss, "The equilibrium structure and fundamental vibrational frequencies of dioxirane," J. Chem. Phys. 108, 7190-7196 (1998).
- ⁹⁸W. Schneider and W. Thiel, "Anharmonic force fields from analytic second derivatives: Method and application to methyl bromide," Chem. Phys. Lett. **157**, 367–373 (1989).
- ⁹⁹I. M. Mills, "Vibration-rotation structure in asymmetric- and symmetric-top molecules," in *Molecular Spectroscopy: Modern Research*, edited by K. N. Rao and C. W. Mathews (Academic Press, New York, 1972), Vol. 1, pp 115–140.
- ¹⁰⁰C. Puzzarini, J. Bloino, N. Tasinato, and V. Barone, "Accuracy and interpretability: The devil and the holy grail. New routes across old boundaries in computational spectroscopy," Chem. Rev. 119, 8131–8191 (2019).
- 101 J. W. Williams and C. D. Hurd, "An improved apparatus for the laboratory preparation of ketene and butadiene," J. Org. Chem. 5, 122–125 (1940).
 102 P. J. Paulsen and W. D. Cooke, "Preparation of deuterated solvents for nuclear
- ¹⁰²P. J. Paulsen and W. D. Cooke, "Preparation of deuterated solvents for nuclear magnetic resonance spectrometry," Anal. Chem. 35, 1560 (1963).
- ¹⁰³J. K. G. Watson, "Determination of centrifugal distortion coefficients of asymmetric-top molecules," J. Chem. Phys. 46, 1935–1949 (1967).
- 104G. Winnewisser, "Millimeter wave rotational spectrum of HSSH and DSSD. II. Anomalous *K* doubling caused by centrifugal distortion in DSSD," J. Chem. Phys. 56, 2944–2954 (1972).
- ¹⁰⁵B. P. van Eijck, "Reformulation of quartic centrifugal distortion Hamiltonian," J. Mol. Spectrosc. 53, 246–249 (1974).
- ¹⁰⁶V. Typke, "Centrifugal distortion analysis including P⁶-terms," J. Mol. Spectrosc. 63, 170–179 (1976).
- 1^{ô7}L. Margulès, A. Perrin, J. Demaison, I. Merke, H. Willner, M. Rotger, and V. Boudon, "Breakdown of the reduction of the rovibrational Hamiltonian: The case of S¹⁸O₂F₂," J. Mol. Spectrosc. **256**, 232–237 (2009).
- ¹⁰⁸R. A. Motiyenko, L. Margulès, E. A. Alekseev, J.-C. Guillemin, and J. Demaison, "Centrifugal distortion analysis of the rotational spectrum of aziridine: Comparison of different Hamiltonians," J. Mol. Spectrosc. 264, 94–99 (2010).
- ¹⁰⁹J. Doose, A. Guarnieri, W. Neustock, R. Schwarz, F. Winther, and F. Hegelund, "Application of a PC-controlled MW-spectrometer for the analysis of ketene-D₂. Simultaneous analysis of vibrational excited states using microwave and infrared spectra," Z. Naturforsch., A: Phys. Sci. 44, 538–550 (1989).
- ¹¹⁰K. Vávra, P. Kania, J. Koucký, Z. Kisiel, and Š. Urban, "Rotational spectra of hydrazoic acid," J. Mol. Spectrosc. 337, 27–31 (2017).
- ¹¹¹A. G. Császár, J. Demaison, and H. D. Rudolph, "Equilibrium structures of three-, four-, five-, six-, and seven-membered unsaturated *N*-containing heterocycles," J. Phys. Chem. A **119**, 1731–1746 (2015).
- ¹¹²R. K. Bohn, J. A. Montgomery, Jr., H. H. Michels, and J. A. Fournier, "Second moments and rotational spectroscopy," J. Mol. Spectrosc. **325**, 42–49 (2016)